Imaging of muscle edema

Poster No.:	C-0841
Congress:	ECR 2016
Type:	Scientific Exhibit
Authors:	M. Eyselbergs, F. M. H. M. Vanhoenacker, M. Faure, J. Huyskens, P. M. Parizel; Antwerp/BE
Keywords:	Edema, Imaging sequences, Ultrasound, CT, MR, Musculoskeletal system
DOI:	10.1594/ecr2016/C-0841

Aims and objectives

Muscle edema is characterized by an increase in free water content. It can occur as a consequence of numerous causes. MRI is the most powerful technique to detect ME using fat suppressed (FS) T2-weighted images (WI) or STIR sequences. ME can be subdivided according to distribution of the lesions. Diffuse (bilateral muscle involvement), focal (one or a contiguous group of muscles involvement) and multifocal (involvement of multiple remote muscles) ME patterns can be distinguished (Fig. 1 on page 2). There is an extremely wide variety of causes often with a characteristic (clinical) feature (Table 1 on page 2, Table 2 on page 3 and Table 3 on page 3).

The objectives of this study are twofold: (1) to retrospectively determine the most frequent etiology of ME and distribution of the ME pattern in a non academic hospital; (2) to present a pictorial overview of the ME pattern encountered in our series and to illustrate the complementary value of FS T2- and T1-WI.

Images for this section:

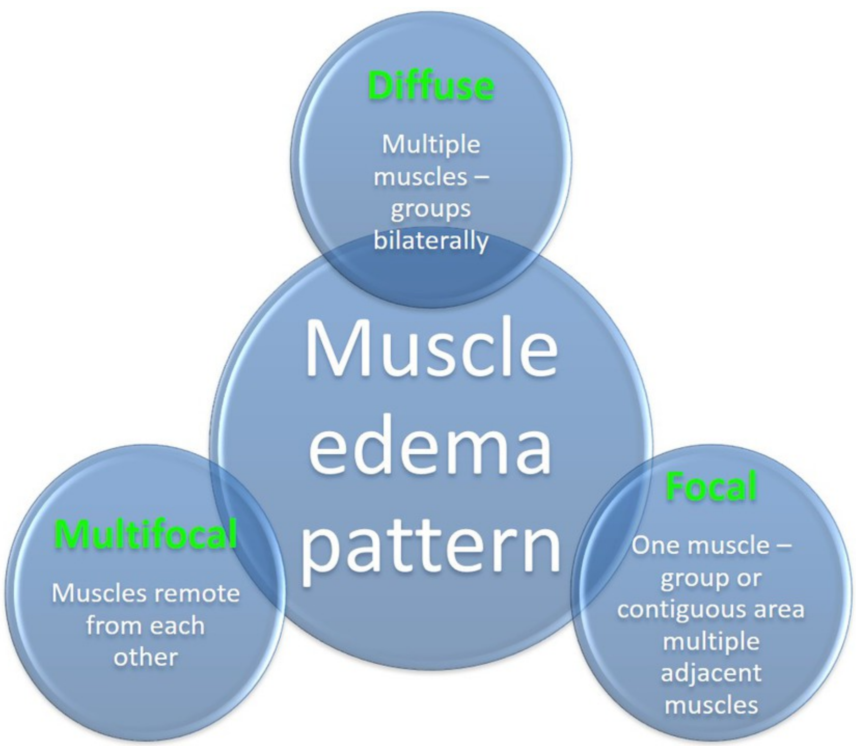

Fig. 1: Subdivison of the muscle edema pattern according to the distribution of the lesions

Causes	Characteristic (clinical) feature
Polymyositis – Dermatomyositis	Proximal distribution, lower more than upper limbs
Inclusion body myositis	Distal distribution
Viral myositis	Systemic symptoms of viral infection
Medication-induced myopathy	Statins, diuretics, zidovudine, amphotericine B, ...

Table 1: Diffuse muscle edema pattern: differential diagnoses and characteristic features

Causes	Characteristic (clinical) features
Myositis	
Strain - rupture - myositis ossificans	Musculotendinous junction
Contusion	Muscle bone interface
Laceration	Linear defect or overlying soft tissue defect
Pyomyositis	Rim-enhancing abscess
Fracture	History of trauma
Necrotizing fasciitis	Gas or rim-enhancing abscesses, contiguous muscle groups
Diabetic muscle infarction	Non-enhancing infarcted muscle, perifascial fluid, lower limbs more frequently involved
Compartment syndrome	Confined to a muscle compartment, non enhancing muscles due to infarction
Denervation	Muscle distribution supplied by a given nerve
Radiation	Along distribution of radiation field
Primary tumor	Enhancing mass - history
Delayed onset muscle soreness	Follows pattern of overuse
Metastasis	Enhancing mass

Table 2: Focal muscle edema pattern: differential diagnoses and characteristic features

Causes	Characteristic (clinical) feature
Delayed onset muscle soreness	Follows pattern of muscle overuse
Pyomyositis	Rim-enhancing abscesses
Sarcoid myopathy: nodular subtype	Multiple nodules of muscle edema involving multiple muscle groups
Denervation	Muscle distribution supplied by a given nerve
Metastasis	Multiple enhancing masses

Table 3: Mulifocal muscle edema pattern: differential diagnoses and characteristic features

Methods and materials

From June 2005 until February 2012, 13800 musculoskeletal MR examinations were performed in our institution of which 2364 MR studies were included in the scientific database of a non academic hospital (AZ Sint Maarten, Duffel-Mechelen). Every MR study was labelled with a radiological diagnosis and/or specific keyword(s). ME was evaluated on (FS) T2-WI. Atrophy and fatty infiltration were evaluated on T1-WI. In our series, 116 cases were identified on FS T2-WI, 9 cases with ultrasound (US), 1 case with US and additional computed tomography (CT) and 1 case with CT only.

Results

Objective 1: to retrospectively determine the most frequent etiology of ME and distribution of the ME pattern in a non academic hospital

The following etiologies were found in our series (Fig. 2 on page 8): traumatic (n = 106), denervation (n = 11), inflammatory (n = 6), infectious (n = 3) and metastasis (n = 1). Proportions were respectively 83%, 9%, 5%, 2% and 1%. The distribution of the ME pattern was the following: diffuse (n = 1), focal (n = 124) and multifocal (n = 2). In all cases of denervation ME (n = 11), there was a variable grade of muscle atrophy and fatty infiltration. T1-WI were most helpful in case of denervation edema and may add additional information regarding chronicity and reversibility.

Objective 2: to present a pictorial review of the ME pattern encountered in our series and to demonstrate the complementary value of FS T2-WI and T1-WI

a) **'Diffuse' ME pattern**

A 55-year-old woman presented with bilateral muscle stiffness around the pelvis and lower extremities. Axial FS T2-WI showed ME in multiple muscle groups such as the pectineus and adductor muscles bilaterally and quadriceps muscle on the left (Fig. 3 on page 9). Combined with clinical and laboratory parameters, the diagnosis of **polymyositis** was made.

b) **'Focal' ME pattern**

A 37-year-old women presented with pain at the dorsal aspect of the right foot. Sagittal FS T2-WI showed ME in the dorsal interosseous muscles between ray 2 and 3, compatible with focal **myositis** (Fig. 4 on page 10).

A 55-year-old man presented with pain in the left mandibular region after a dental procedure. Ultrasound showed a hypoechoic swollen masseter muscle (arrow in Fig. 5 on page 12). Also note the small amount of fluid surrounding the muscle (x-x in Fig. 5 on page 12). Axial CT image confirmed a diffusely swollen and hypodense masseter muscle with surrounding inflammatory changes (arrow in Fig. 6 on page 12), compatible with focal **myositis**.

A 50-year-old woman complained of a focal mass in the right infrascapular region. Ultrasound showed a hypoechoic mass in the latissimus dorsi muscle (Fig. 7 on page 14) with preserved but thickened muscle fibers (asterisks in Fig. 7 on page 14). Axial FS T2-WI showed an intramuscular lesion with peripheral high signal (arrows in Fig. 8 on page 14) and hypointens signal of the centrally located fibres (asterisks in Fig. 8 on page 14). Control ultrasound 4 weeks later showed complete resolution of the lesion (Fig. 9 on page 15). The diagnosis of an **inflammatory pseudotumor** was made.

A 56-year-old man suffered from epicondylitis lateralis (tennis elbow) (arrow in Fig. 10 on page 16) and axial FS T2-WI showed remarkable **reactive ME in the anconeus muscle** as a secondary finding (arrow in Fig. 11 on page 17).

Longer standing **traumatic injury of the left gluteus musculature** with obvious fatty infiltration was clearly appreciated on coronal T1-WI in a 60-year-old man (arrow in Fig. 12 on page 18).

Traumatic ME at the myotendinous junction of the biceps femoris muscle (arrow in Fig. 13 on page 19) after a **sports injury** in a 29-year-old man.

Delayed Onset Muscle Soreness (DOMS) is a type of overuse injury that does not become symptomatic until hours or days after the overuse episode, in contrast with a muscle strain or contusion, which usually is immediately painful. Coronal and axial FS T2-WI showed diffuse ME in the right soleus muscle not solely localized to the myotendinous junction in a 25-year-old professional football player (arrow in Fig. 14 on page 20 and Fig. 15 on page 21). Symptoms developped 1-2 days following exercise and resolved in approximately 2 weeks.

Traumatic ME in the obturator externus and to a lesser extent the obturator internus muscle (arrows on coronal and axial FS T2-WI Fig. 16 on page 22 and Fig. 17 on page 23) secondary to **fractures** of the anterior acetabulum (arrow in Fig. 18 on page 24) and lower pubic bone (arrow in Fig. 19 on page 25) in a 55-year-old man.

A 67-year-old woman with a history of esophageal carcinoma complained from pain since three weeks at the left thigh that exacerbated acutely. Coronal FS T2-WI showed extensive ME most prominent in the gluteus musculature (arrow in Fig. 20 on page 26). Axial T1-WI with substraction showed marked enhancement of the musculature due to **metastatic invasion** of the muscles (arrow in Fig. 21 on page 26). Biopsy confirmed the diagnosis.

A 65-year-old woman recently underwent orthopaedic surgery complicated with extensive wound infection at her right upper leg. Coronal FS T2-WI showed marked ME in the upper leg muscles most prominent in the quadriceps muscle (arrow in Fig. 22 on page 27). Contrast enhanced T1-WI clearly demonstrated concomitant abscess formation (arrow in Fig. 23 on page 28). The diagnosis of a focal **pyomyositis** was made. Microbiological investigation confirmed the diagnosis.

Paracoronal (Fig. 24 on page 29) and parasagittal (Fig. 25 on page 30) FS T2-WI showed selective ME in the extensor digitorum brevis muscle of the left foot, a finding consistent with **denervation** after trauma with partial involvement of the deep peroneal nerve in a 37-year-old male recreational soccer player. The common peroneal nerve divides into the superficial and deep peroneal branches. The deep branch supplies the extensor muscles in the anterior compartment of the lower part of the leg, including the tibialis anterior, extensor hallucis longus, and extensor digitorum longus and (more distally) brevis muscles, whereas the superficial branch innervates the peroneus longus and peroneus brevis muscles (Fig. 26 on page 32).

A 36-year-old man presented with sudden onset of a painful shoulder girdle and progressive weakness on the right side. Parasagittal FS T2-WI showed ME in the supra- and infraspinatus muscle (arrows in Fig. 27 on page 34) with concommitant fatty atrophy (arrows in Fig. 28 on page 35) suggestive of longer standing pathology. Direct MR-arthrograpy showed no evidence of a rotator cuff tear (Fig. 29 on page 35). The combination of the history, EMG (demonstrating denervation changes especially of the suprascapular nerve) and imaging findings led to the diagnosis of an **acute iodiopathic brachial neuritis** or **Parsonage Turner syndrome**.

c) **'Multifocal' ME pattern**

A 48-year-old woman with no history of trauma presented with pain in the right forearm and loss of flexion at the distal interphalangeal joint of the index finger and interphalangeal joint of the thumb. Increased signal intensity is depicted on FS T2-WI in keeping with ME in the radial half of the flexor digitorum profundus (arrow in Fig. 30 on page 36 and Fig. 31 on page 37), the flexor pollicis longus (double arrow in Fig. 31 on page 37) and the pronator quadratus muscles (arrow in Fig. 32 on page 38). Furthermore, fatty infiltration and atrophy is seen on the T1-WI (arrow in Fig. 33 on page 39). These imaging findings are consistent with subacute to chronic denervation of the anterior interosseous nerve (AIN). No compression or entrapment of the nerve could be demonstrated. Diagnosis of a **complete interosseous syndrome (AIN)** or **Kiloh-Nevin syndrome** was made. The AIN syndrome arises when the AIN is entrapped or compressed in the proximal part of the forearm. The AIN is a motor branch to the deep ventral muscles of the forearm originating from the median nerve approximately 8 cm distal to the lateral epicondyle. This branch innervates the flexor pollicis longus, the radial half of the flexor digitorum profundus and the pronator quadratus muscles (Fig. 34 on page 40). Flexion at the interphalangeal joint of the thumb and the distal interphalangeal joint of the index finger is not possible due to lack of innervation of the flexor pollicis longus or flexor digitorum profundus muscles (Fig. 35 on page 42 and Fig. 36 on page 42). An incomplete AIN syndrome arises when there is selective involvement of nerve bundles that innervate the flexor pollicis longus or the flexor digitorum profundus muscles with or without involvement of the pronator quadratus muscle. Isolated signal changes of the pronator quadratus muscle need to be interpreted with caution. Slight hyperintensity on T2-WI is often seen in asymptomatic individuals. Therefore, the combination of signal intensity changes in different muscles innervated by the AIN is required for the diagnosis.

Images for this section:

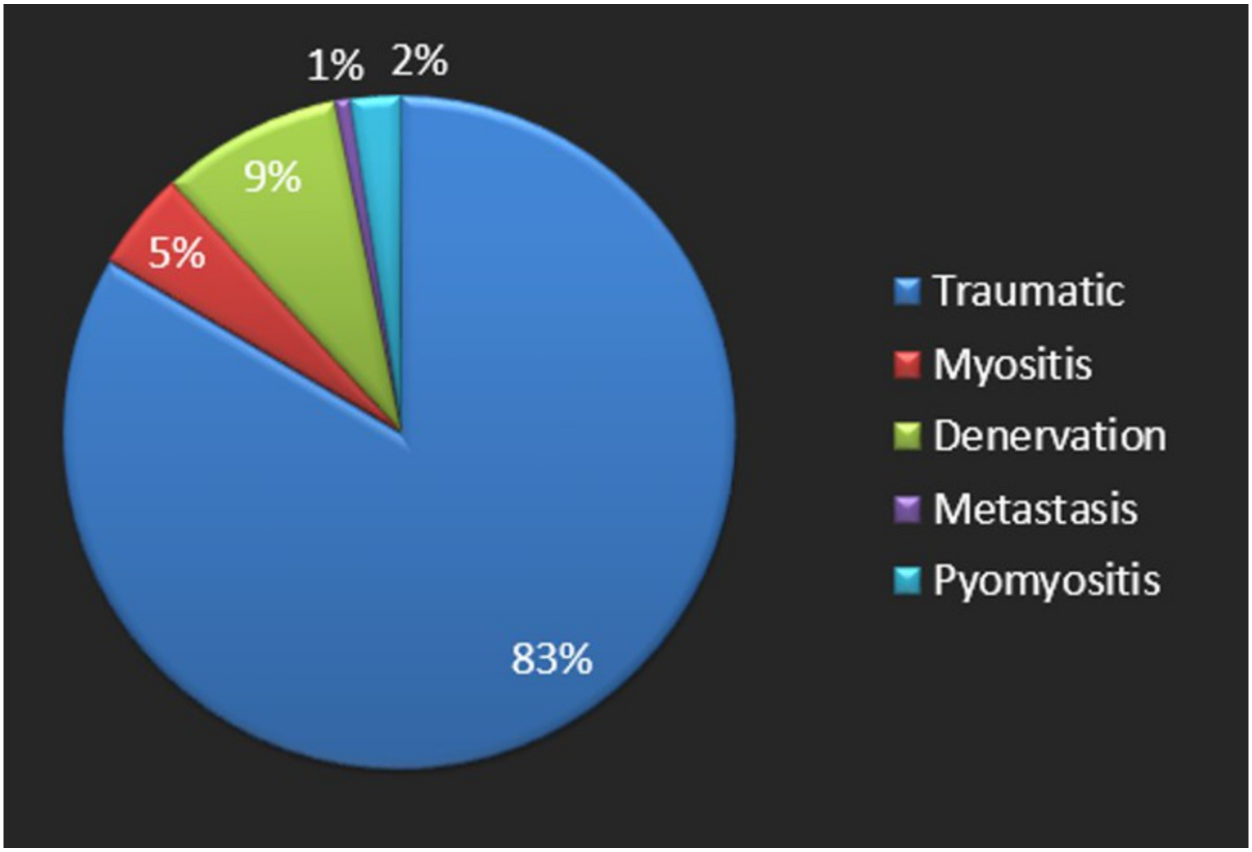

Fig. 2: Schematic overview of the distribution of the different etiologies of muscle edema

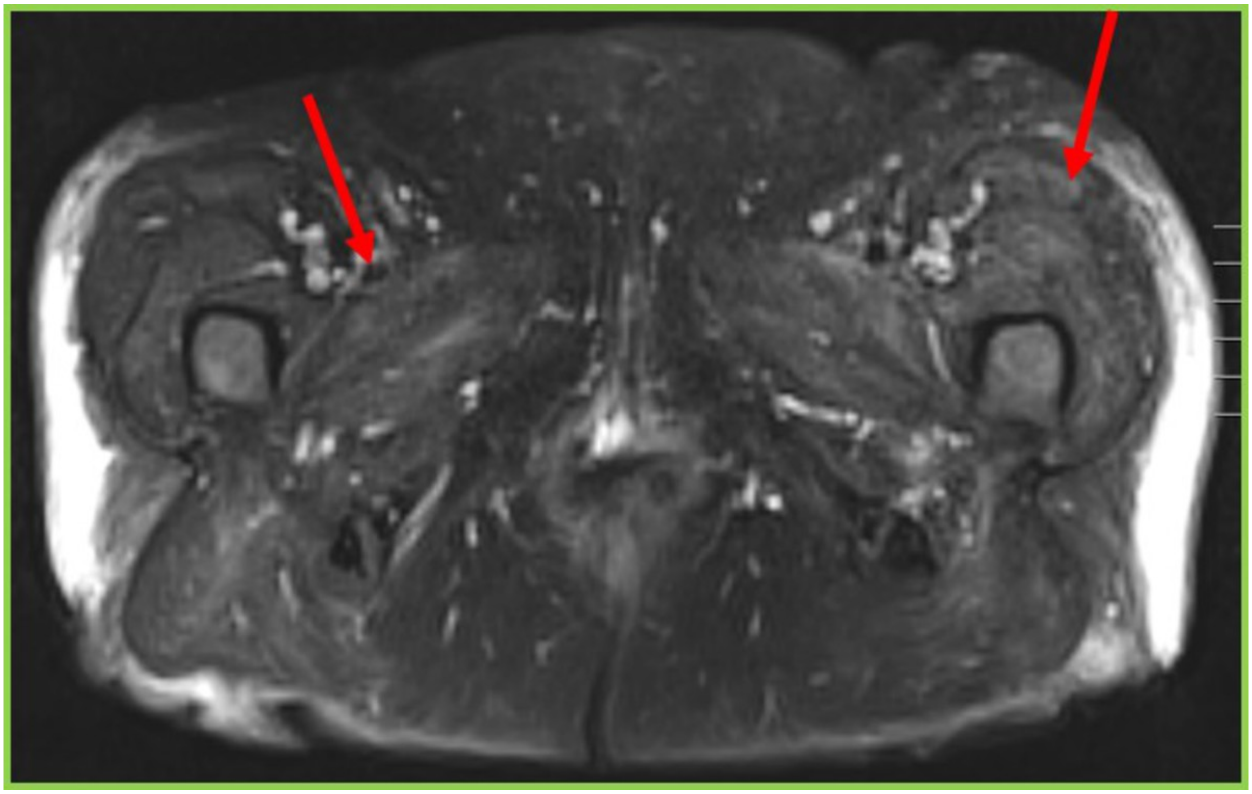

Fig. 3: Axial FS T2-WI showed ME in multiple muscle groups such as the pectineus and adductor muscles bilaterally and quadriceps muscle on the left (arrows)


SPL
t1

Fig. 4: Sagittal FS T2-WI showed ME in the dorsal interosseous muscles between ray 2 and 3 (arrow)

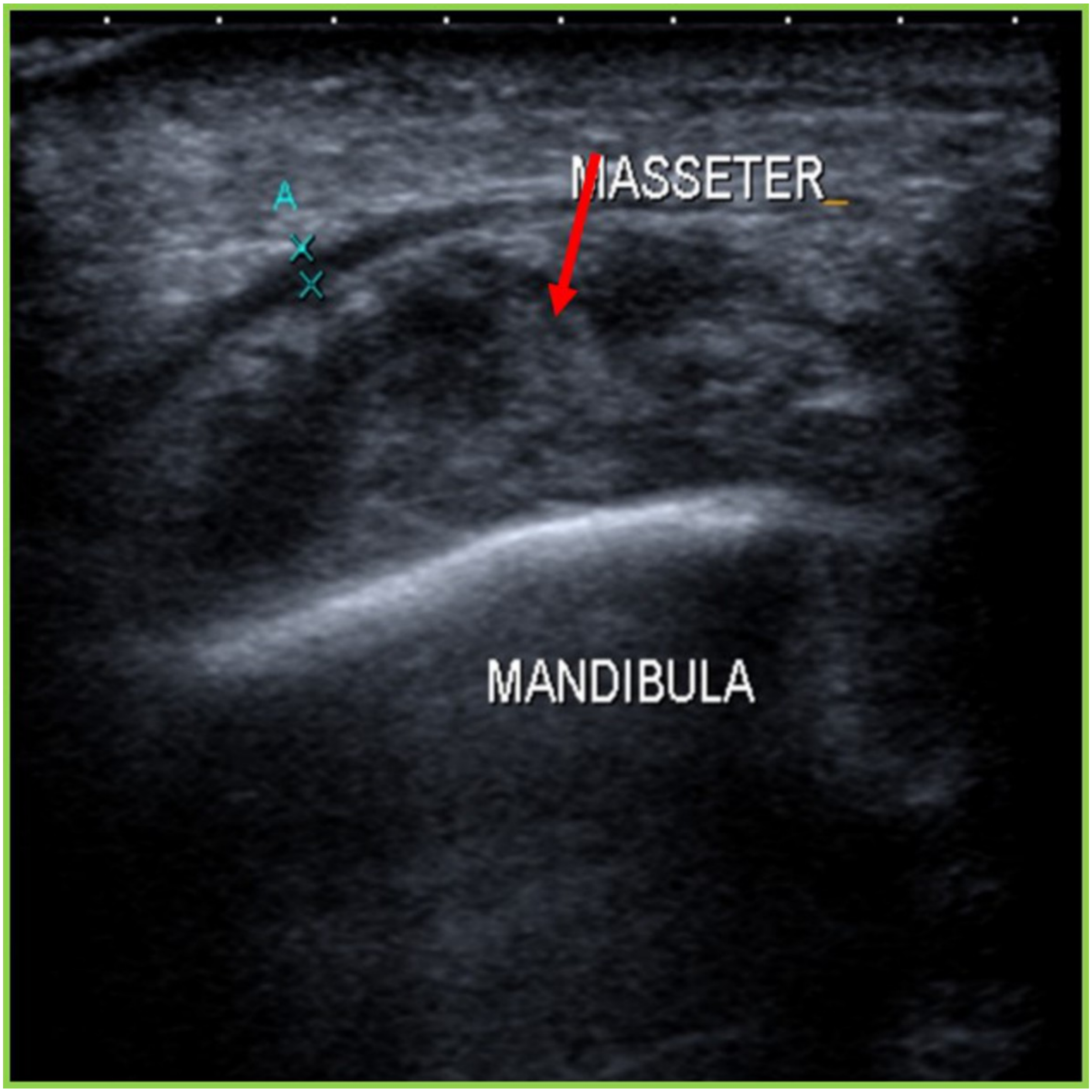

Fig. 5: Ultrasound showed a hypoechoic swollen masseter muscle (arrow). Also note the small amount of fluid surrounding the muscle (x-x)

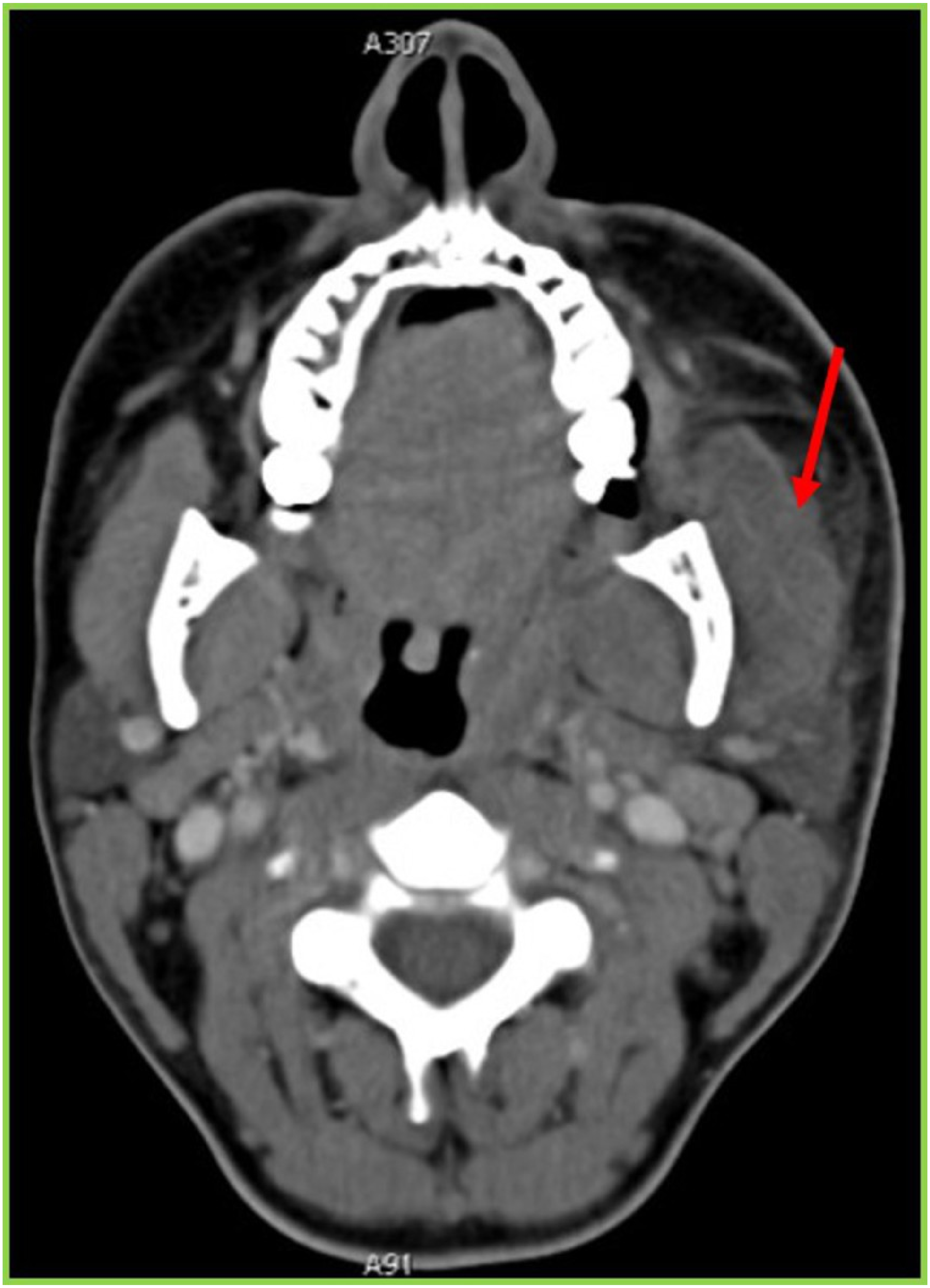
A307
A91

Fig. 6: Axial CT image confirmed a diffusely swollen and hypodense masseter muscle with surrounding inflammatory changes (arrow)

© - Antwerp/BE

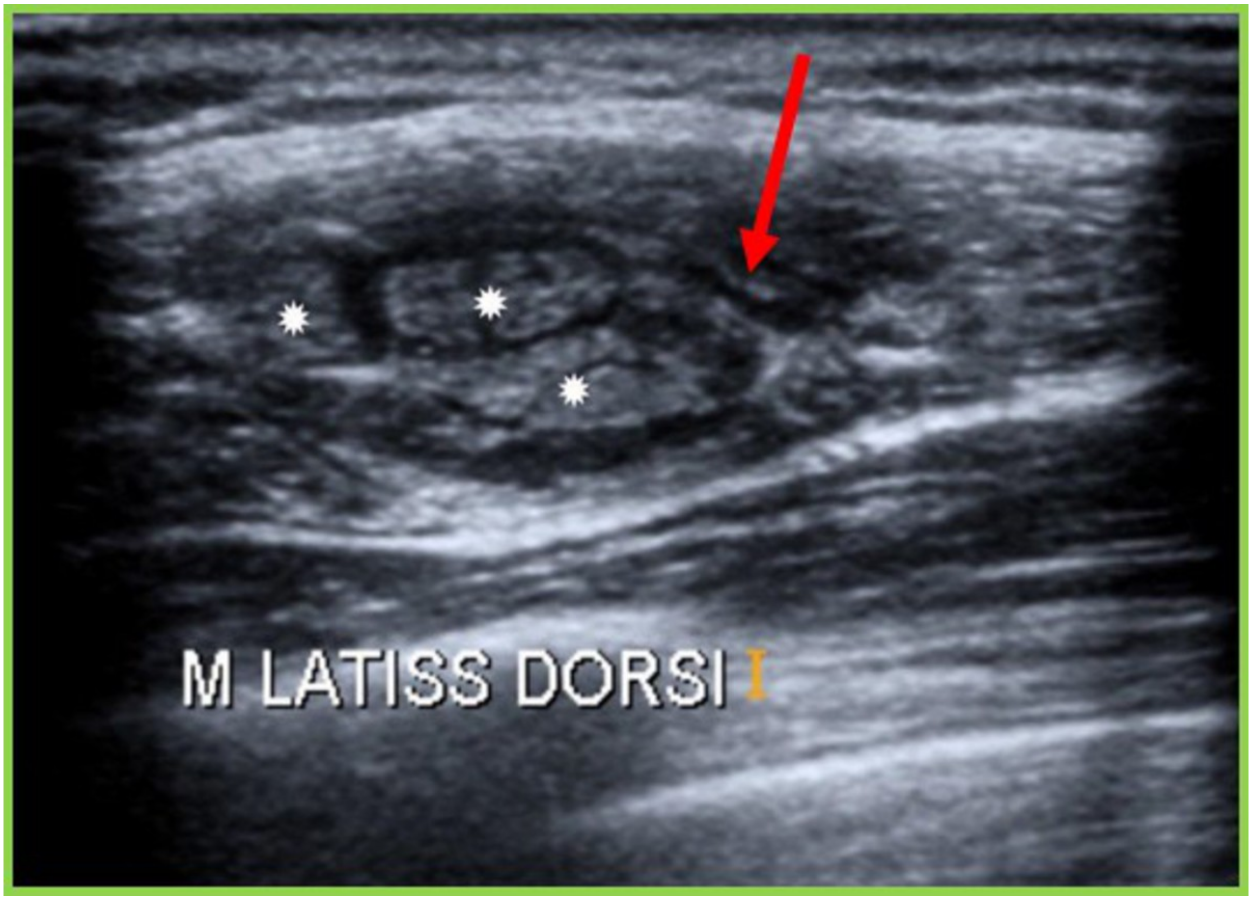

Fig. 7: Ultrasound showed a hypoechoic mass in the right latissimus dorsi muscle (arrow) with preserved but thickened muscle fibers (asterisks)

© - Antwerp/BE

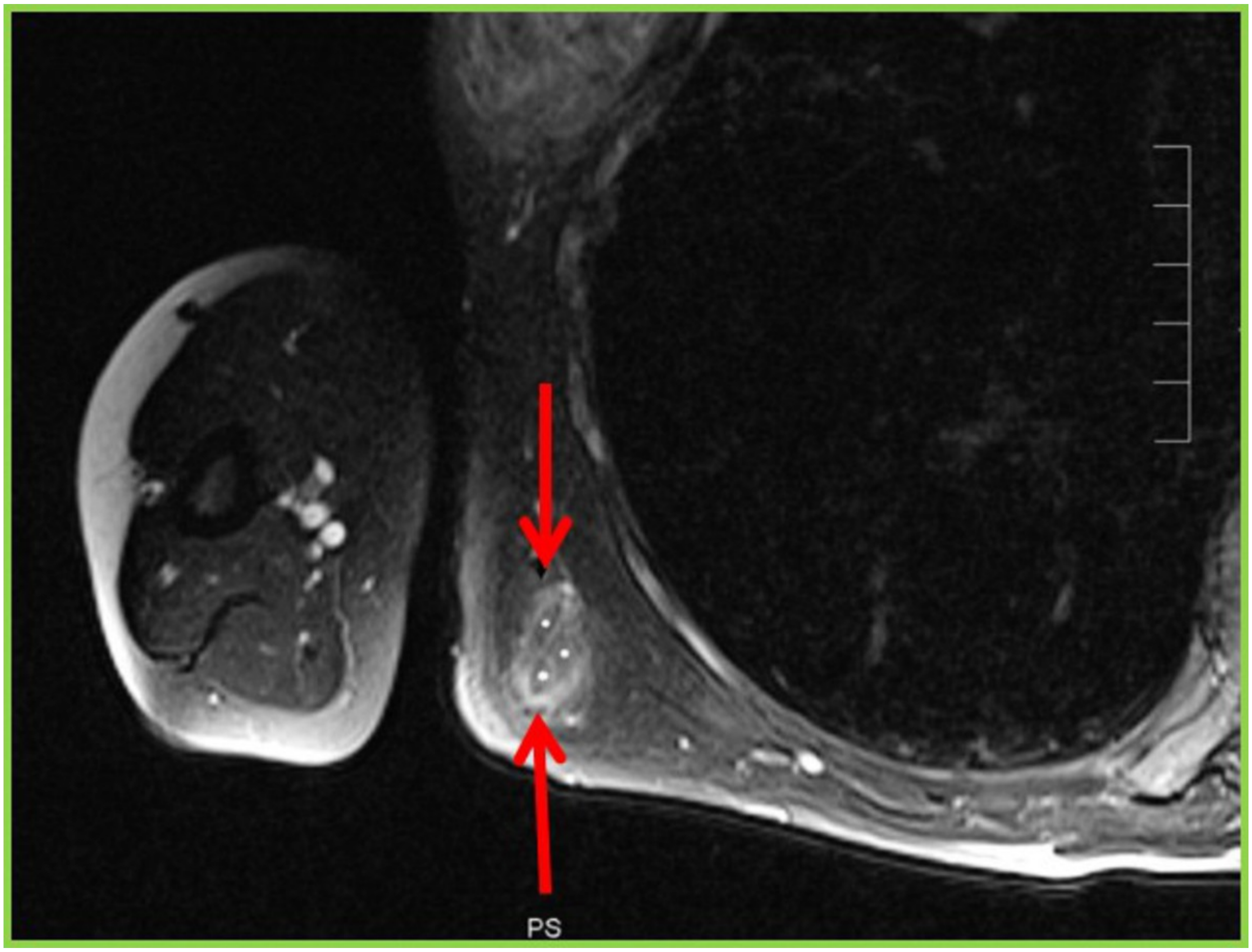

Fig. 8: Axial FS T2-WI showed an intramuscular lesion with high peripheral signal (arrows) and hypointens signal of the centrally located fibres (asterisks)

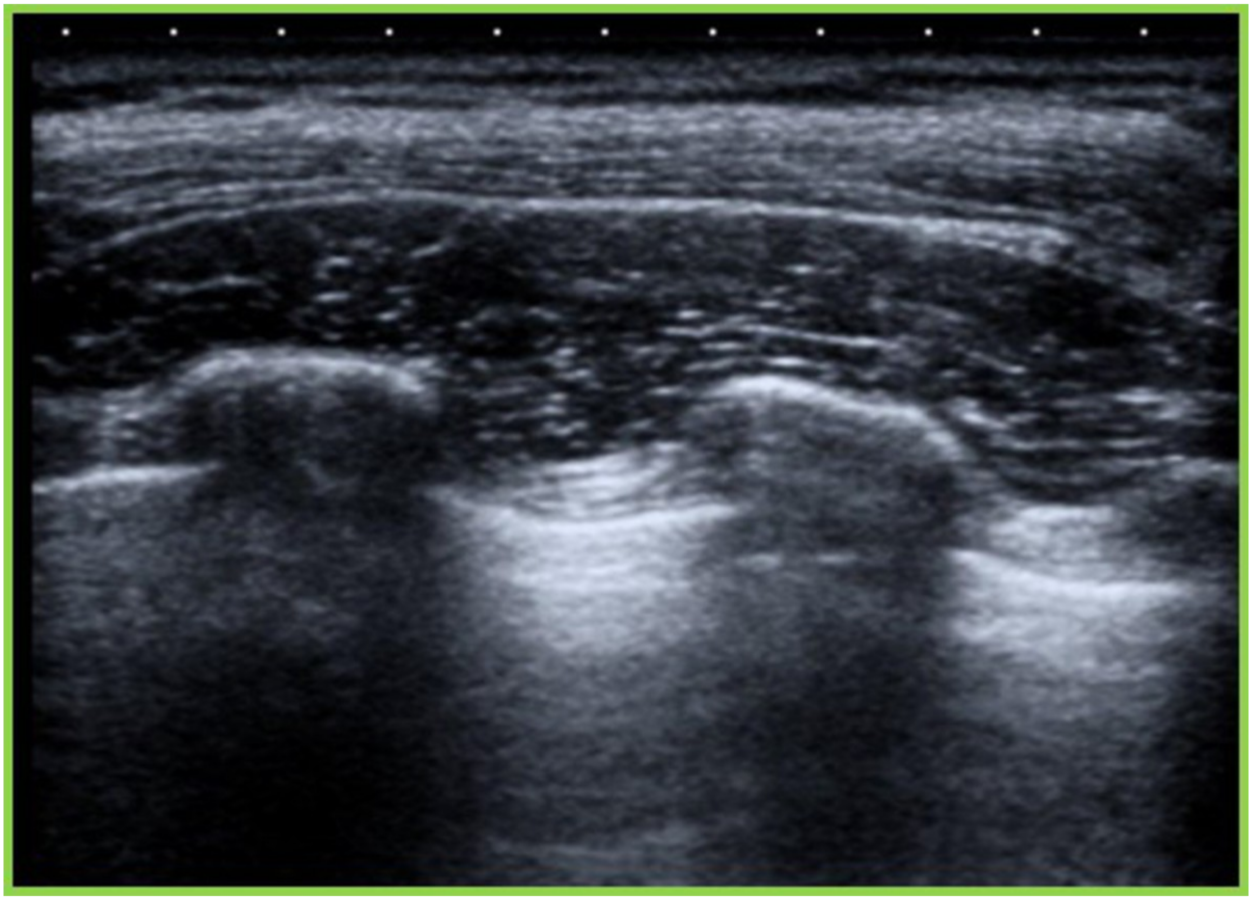

Fig. 9: Control ultrasound 4 weeks later showed complete resolution of the lesion

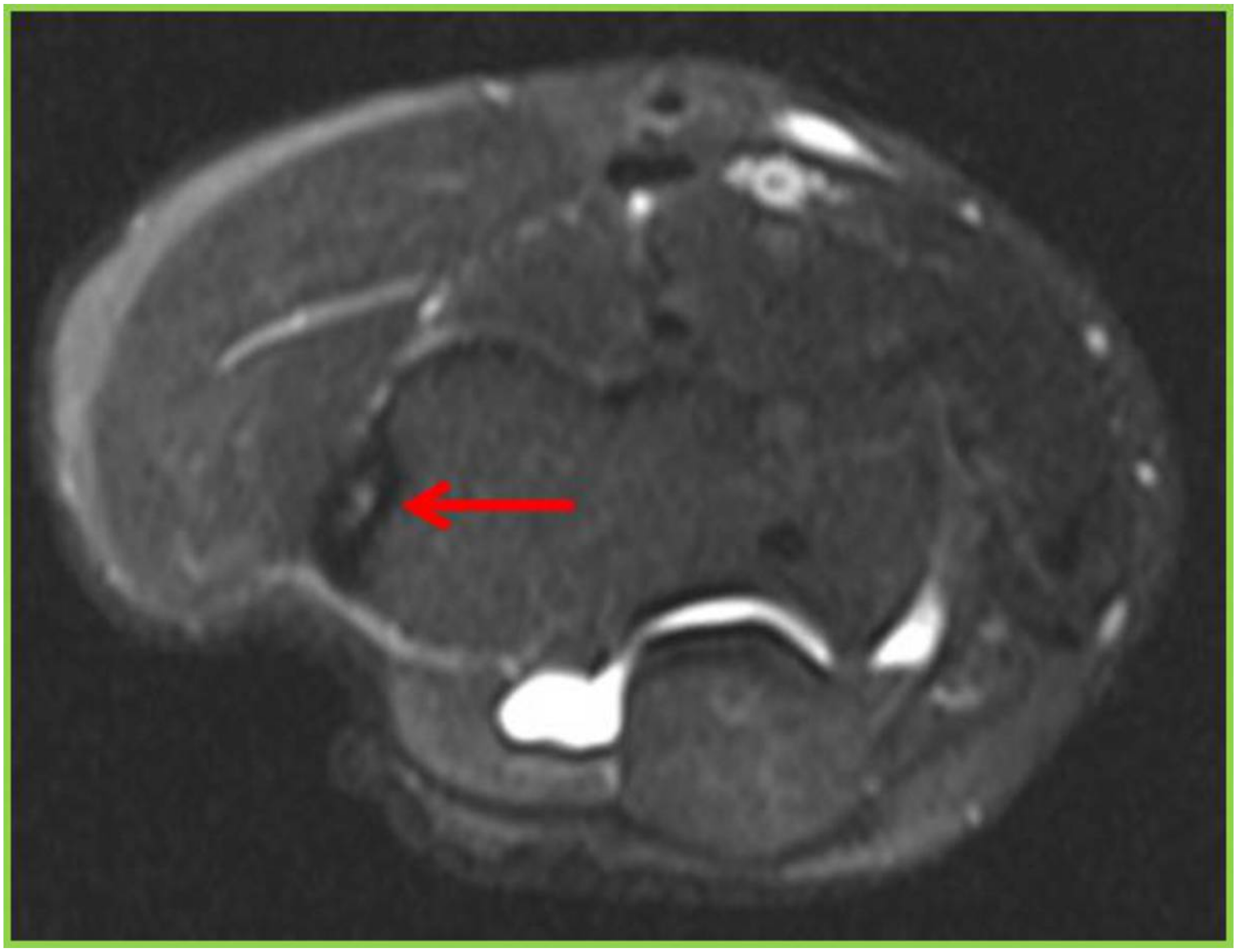

Fig. 10: Axial FS T2-WI showed hyperintense signal in the origin of the common extensor tendon (arrow) compatible with epicondylitis lateralis

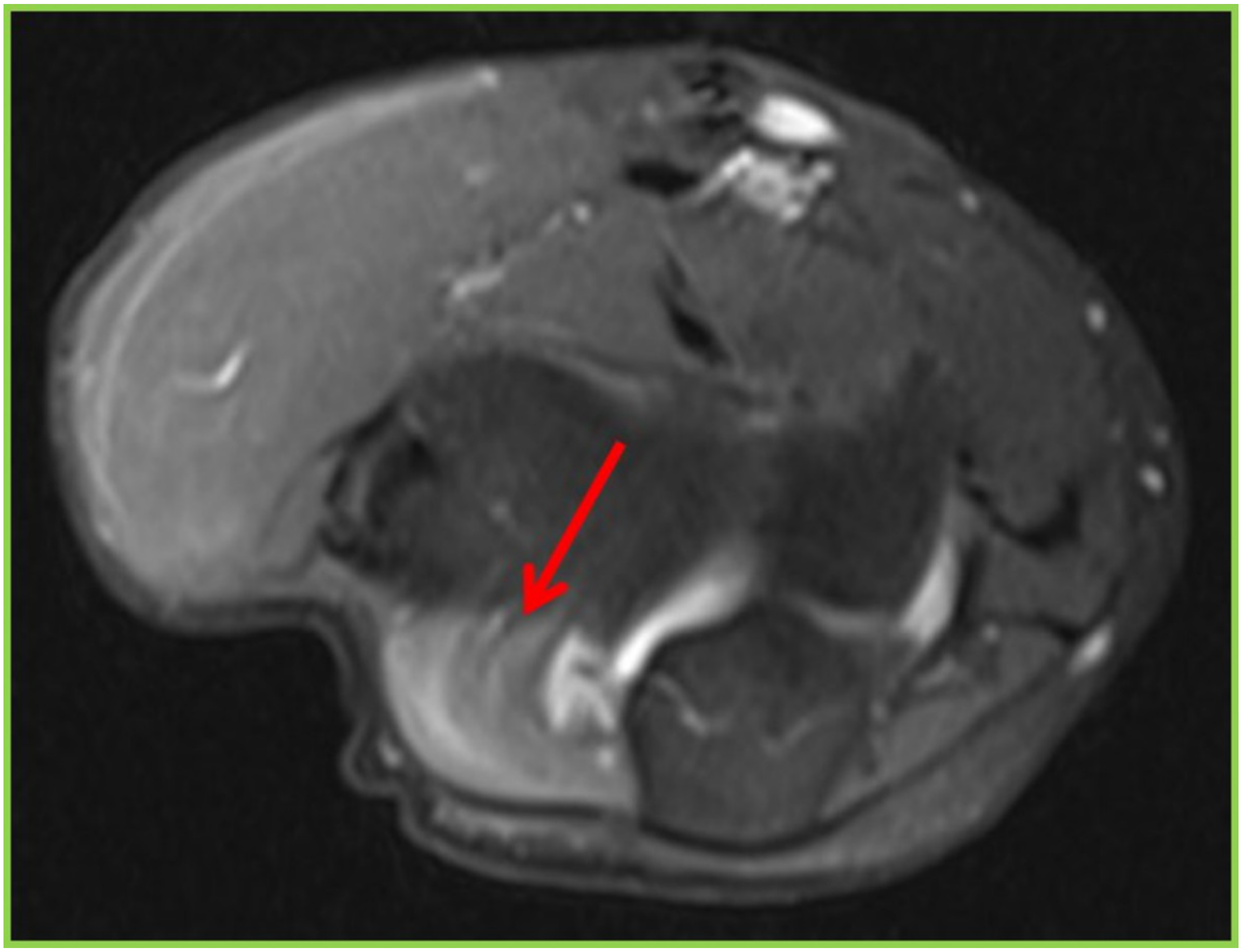

Fig. 11: Axial FS T2-WI showed remarkable ME in the anconeus muscle (arrow)

Fig. 12: Longer standing traumatic injury of the left gluteus musculature with fatty infiltration was clearly appreciated on coronal T1-WI (arrow)

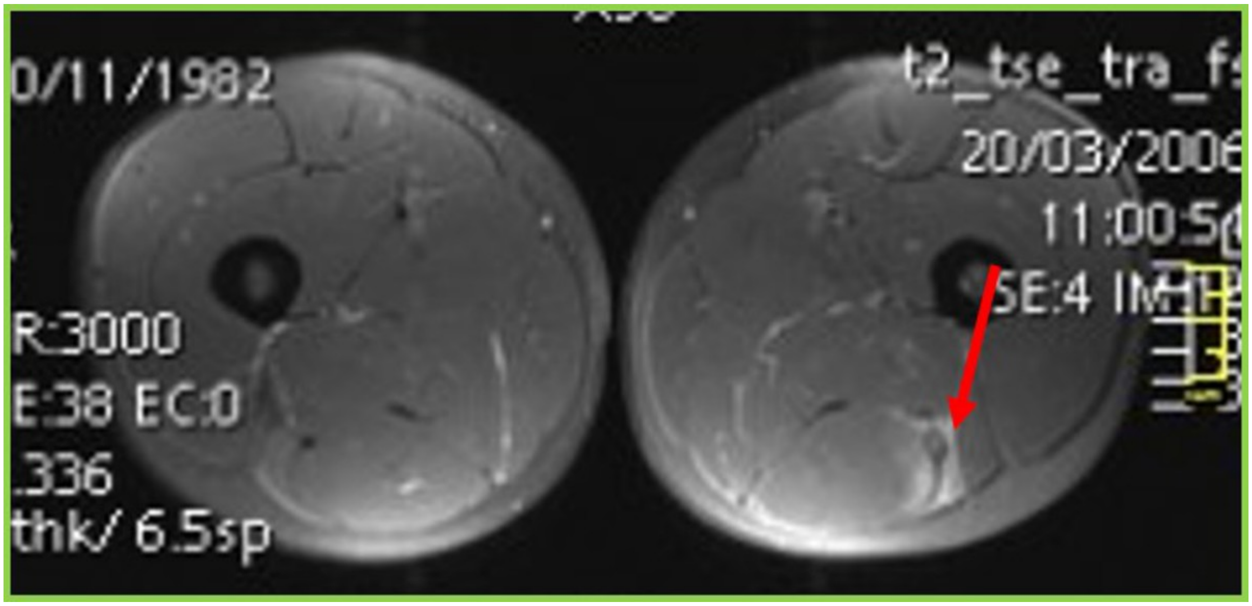

Fig. 13: Axial FS T2-WI showed traumatic ME at the myotendinous junction of the left biceps femoris muscle (arrow)

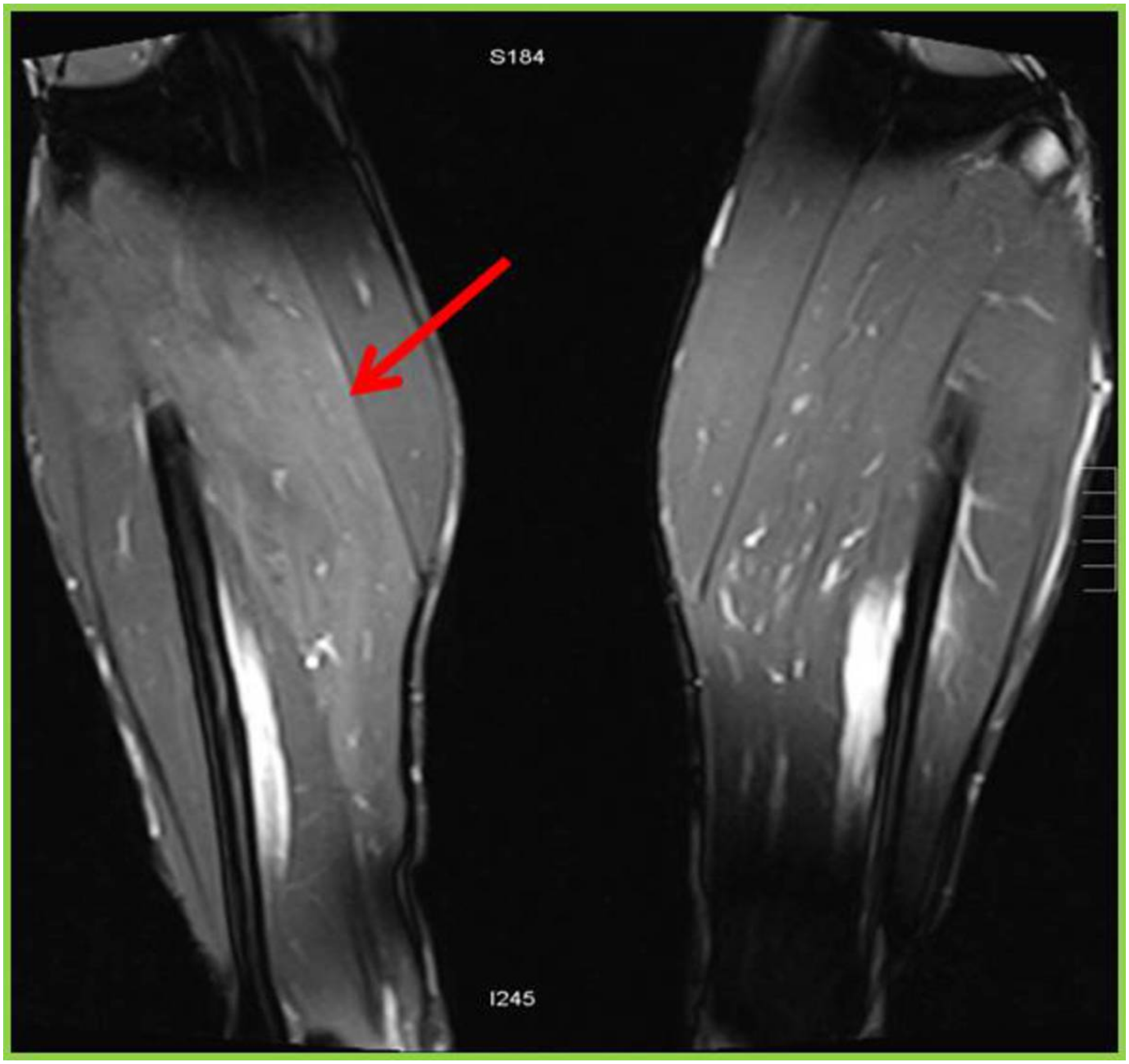

Fig. 14: Coronal FS T2-WI showed diffuse ME in the right soleus muscle not solely localized to the myotendinous junction (arrow)

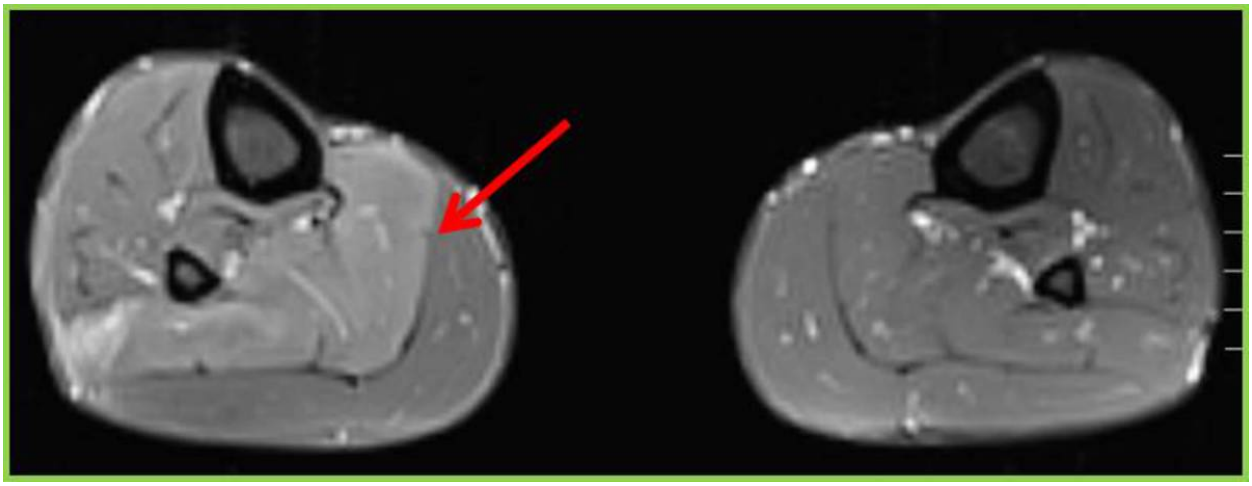

Fig. 15: Axial FS T2-WI showed diffuse ME in the right soleus muscle not solely localized to the myotendinous junction (arrow)

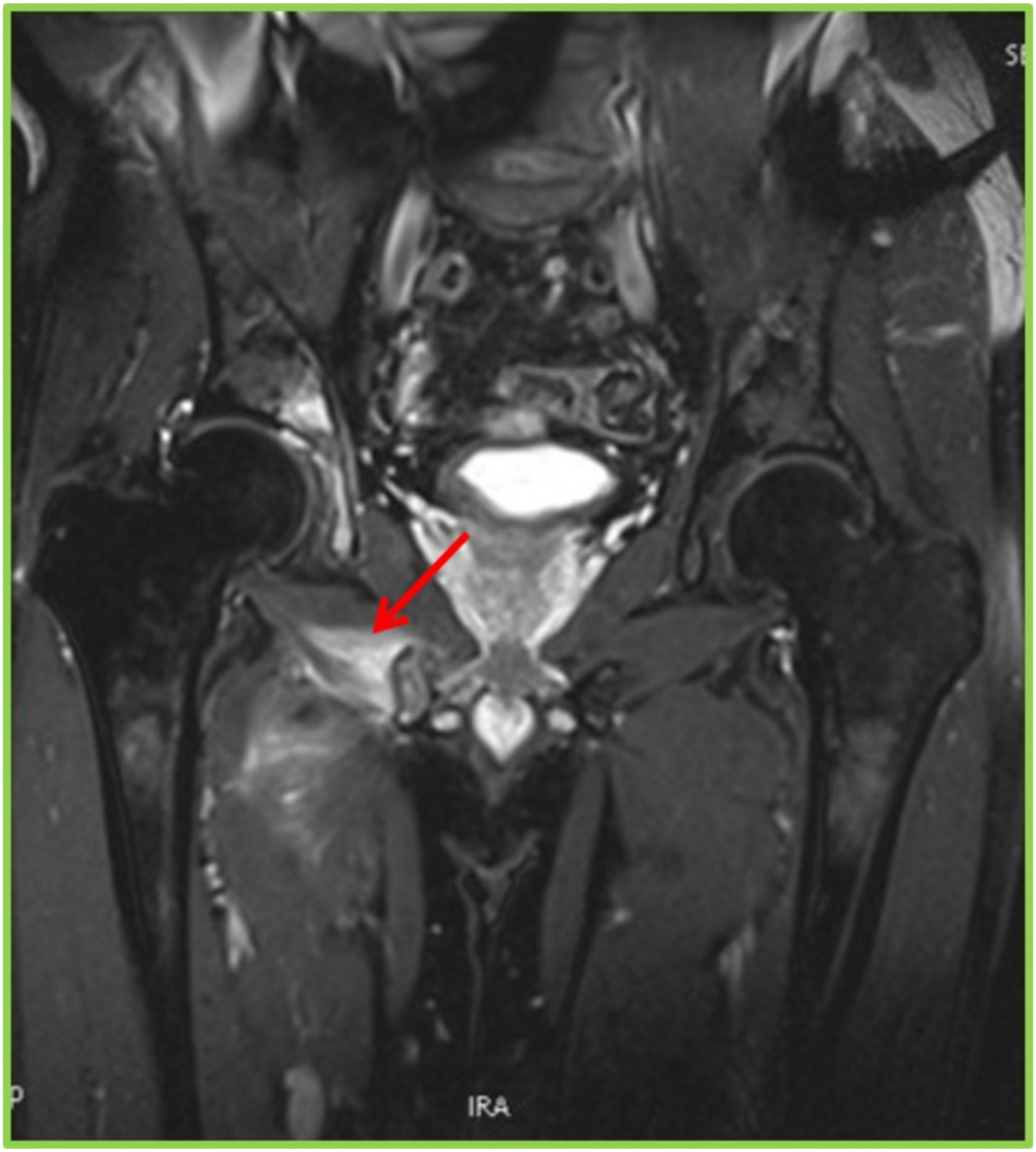

Fig. 16: Traumatic ME in the obturator externus and to a lesser extent the obturator internus muscle (arrow) on coronal FS T2-WI secondary to fractures of the anterior acetabulum and inferior pubic bone

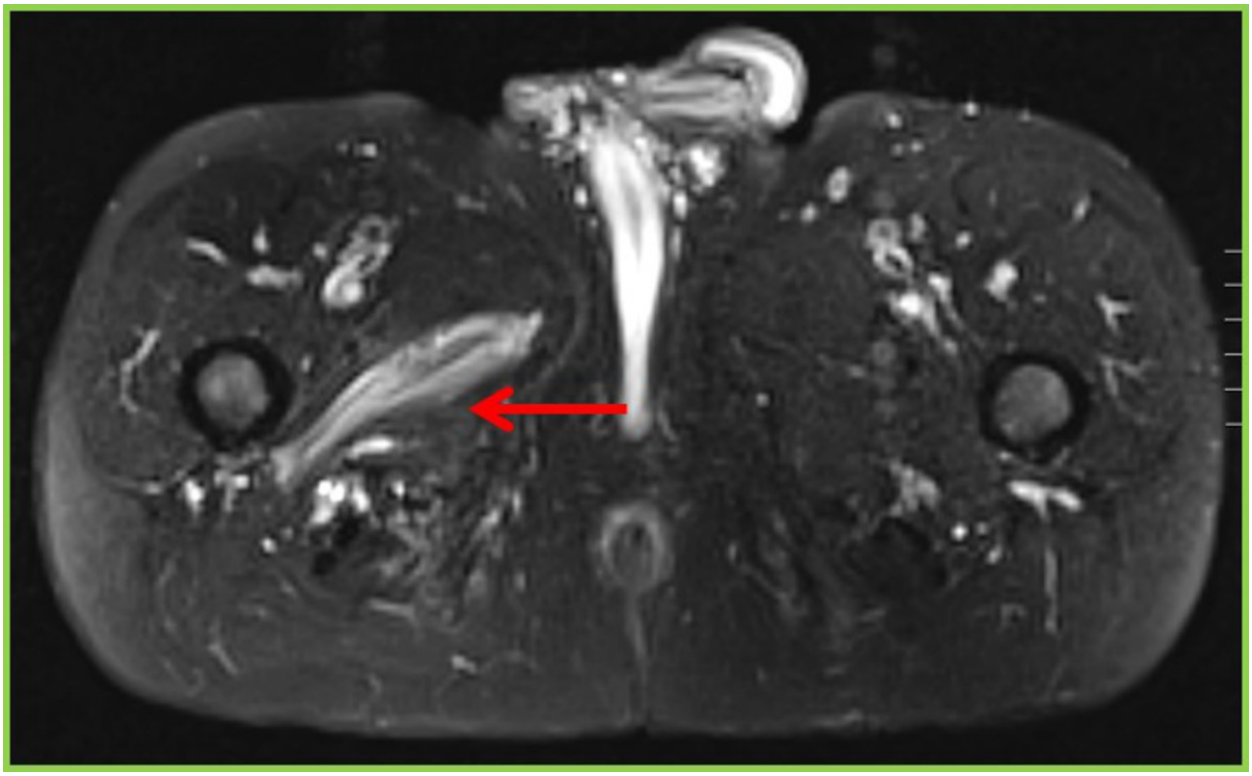

Fig. 17: Traumatic ME in the obturator externus and to a lesser extent the obturator internus muscle (arrow) on axial FS T2-WI secondary to fractures of the anterior acetabulum and inferior pubic bone

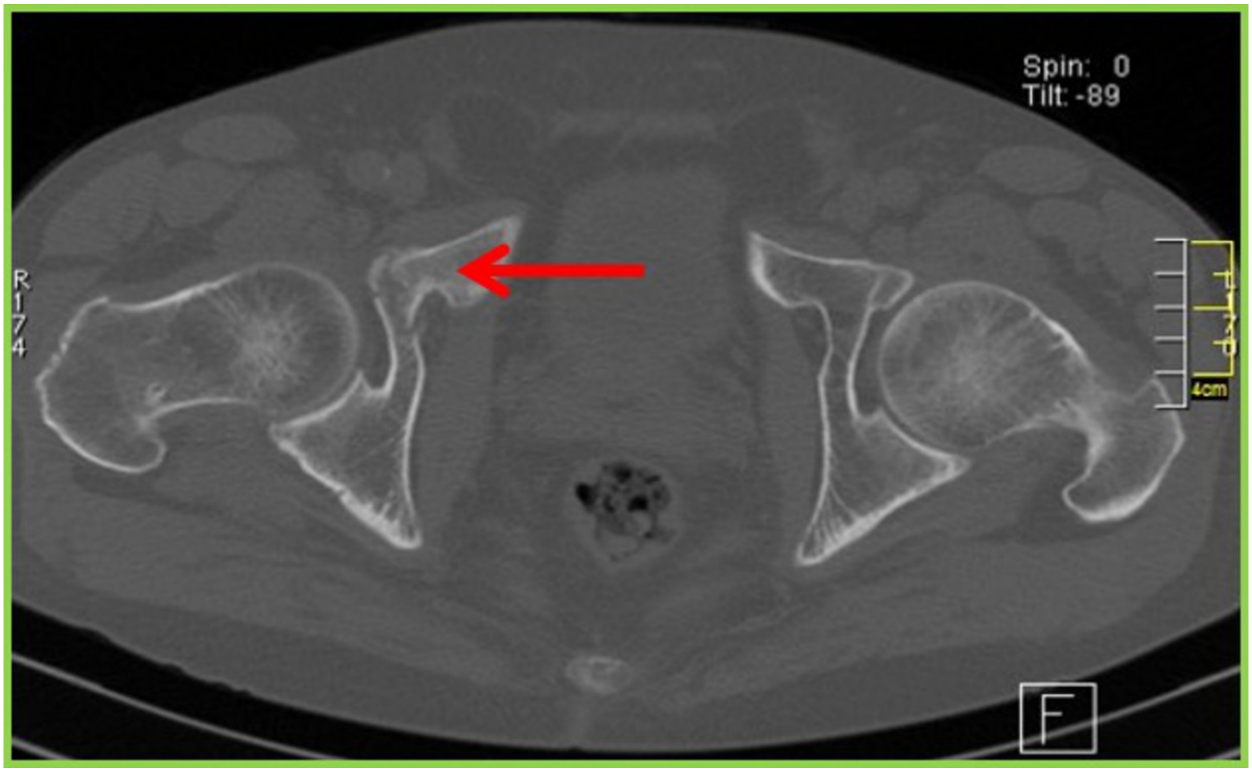

Fig. 18: Axial CT image showed fractures of the anterior acetabulum (arrow) and inferior pubic bone

© - Antwerp/BE

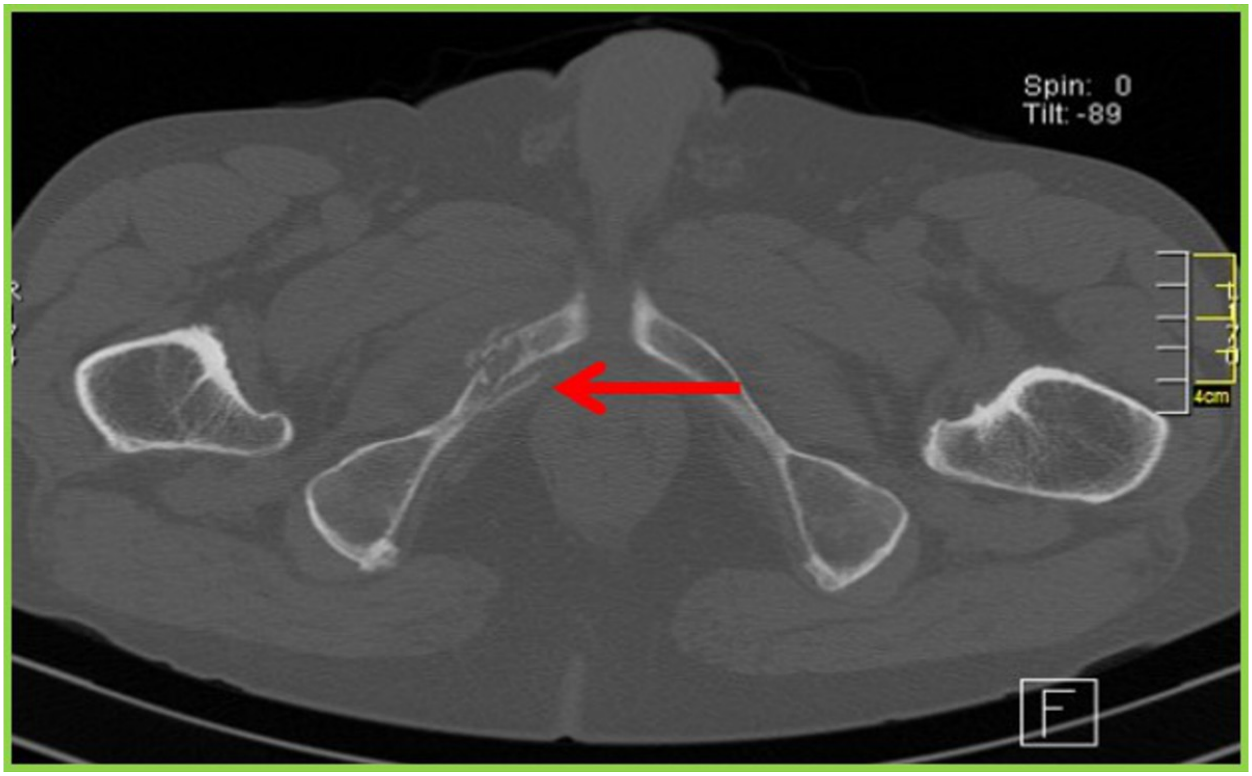

Fig. 19: Axial CT image showed fractures of the anterior acetabulum and inferior pubic bone (arrow)

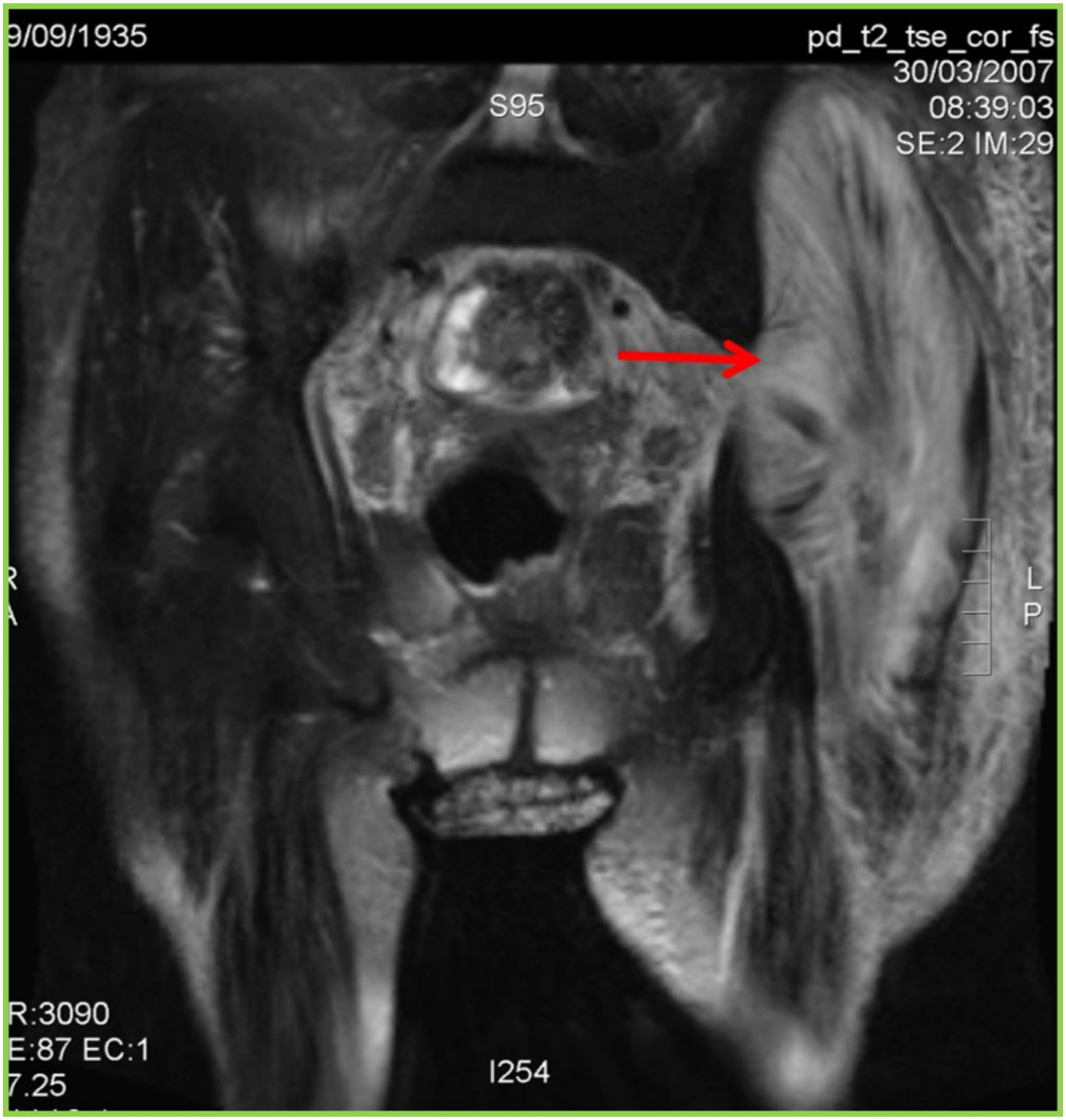

Fig. 20: Coronal FS T2-WI showed extensive ME most prominent in the gluteus musculature (arrow)

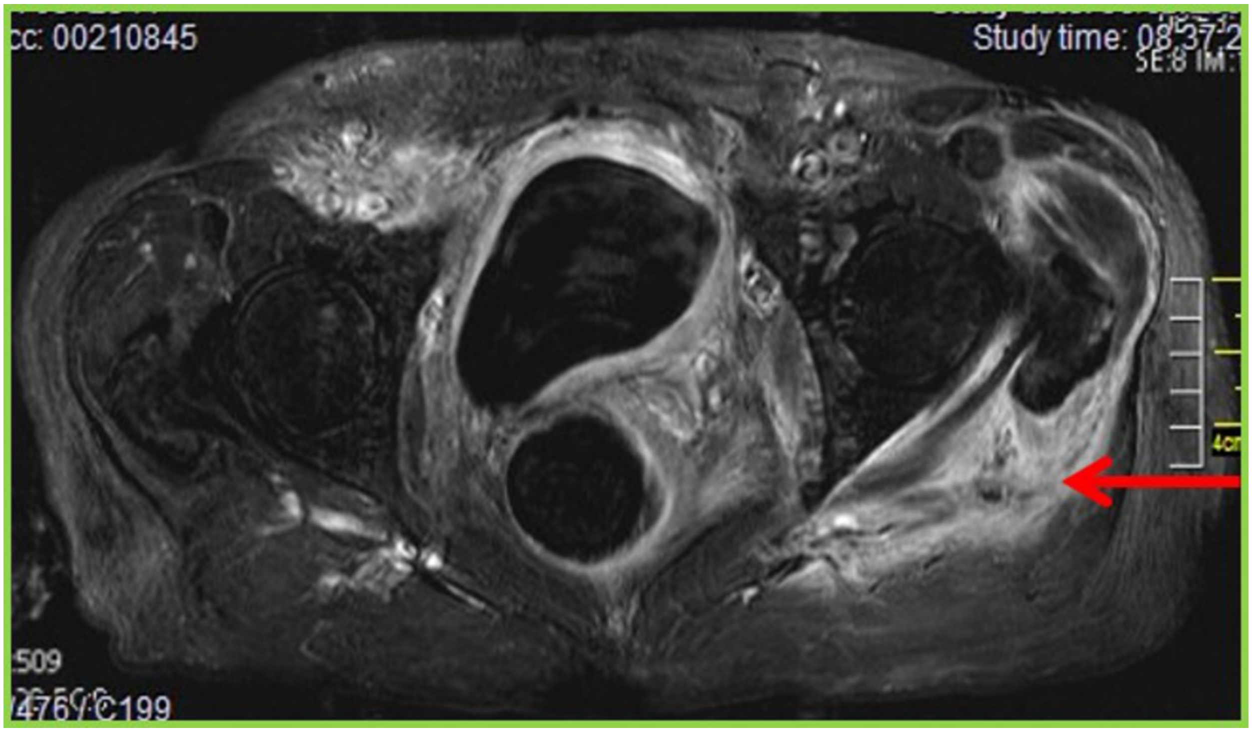

Fig. 21: Contrast enhanced axial T1-WI with subsequent substraction showed marked enhancement of the musculature due to metastatic invasion of the muscles (arrow)

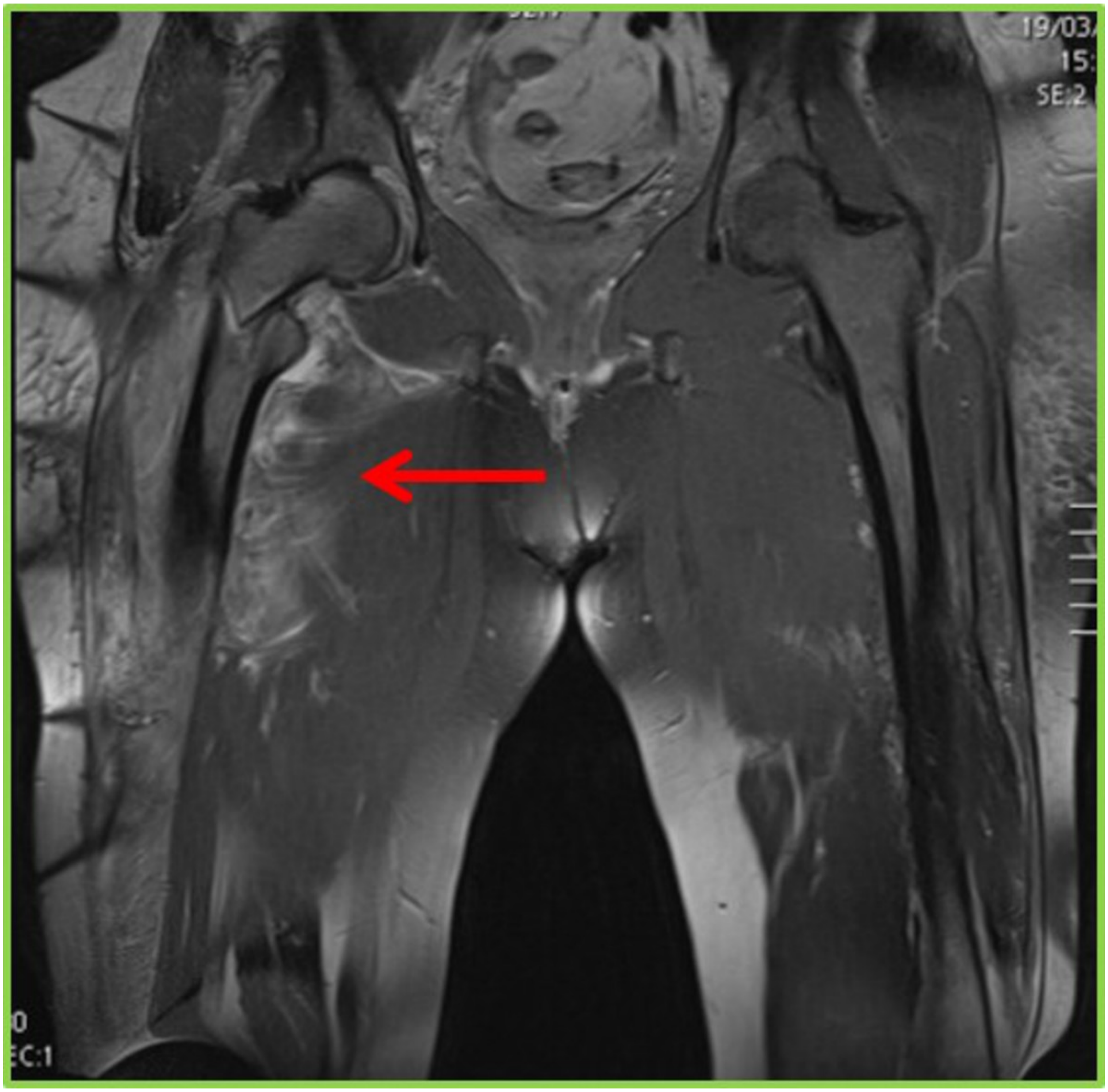

Fig. 22: Coronal FS T2-WI showed marked ME in the right upper leg muscles most prominent in the quadriceps muscle (arrow)

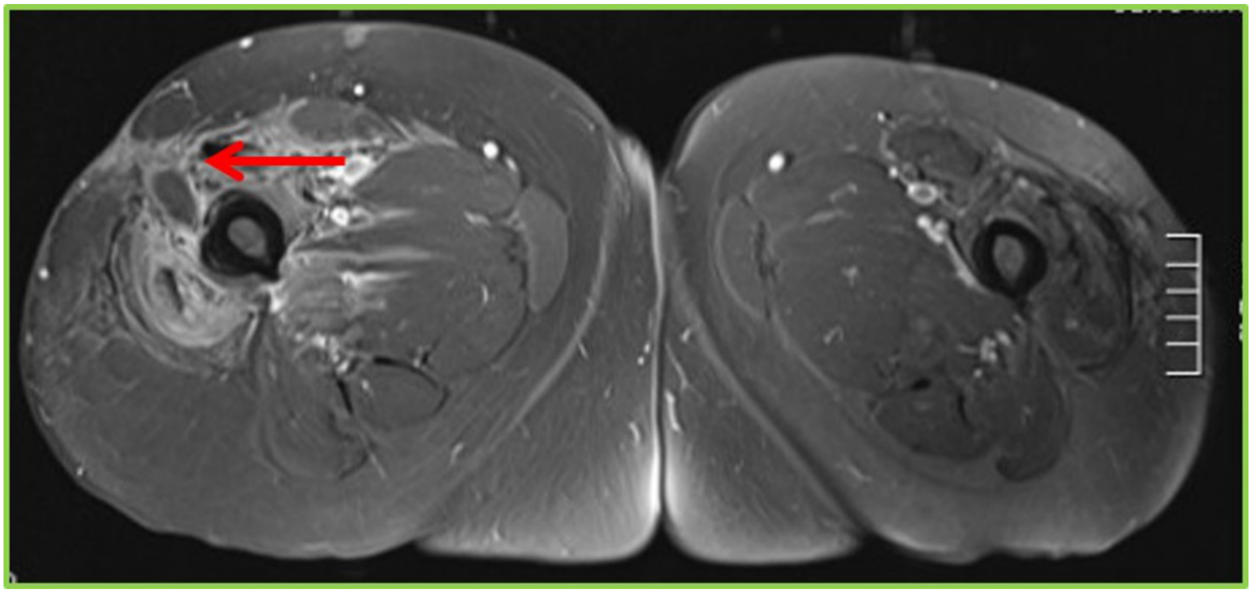

Fig. 23: Contrast enhanced T1-WI clearly demonstrated concomitant abscess formation (arrow)

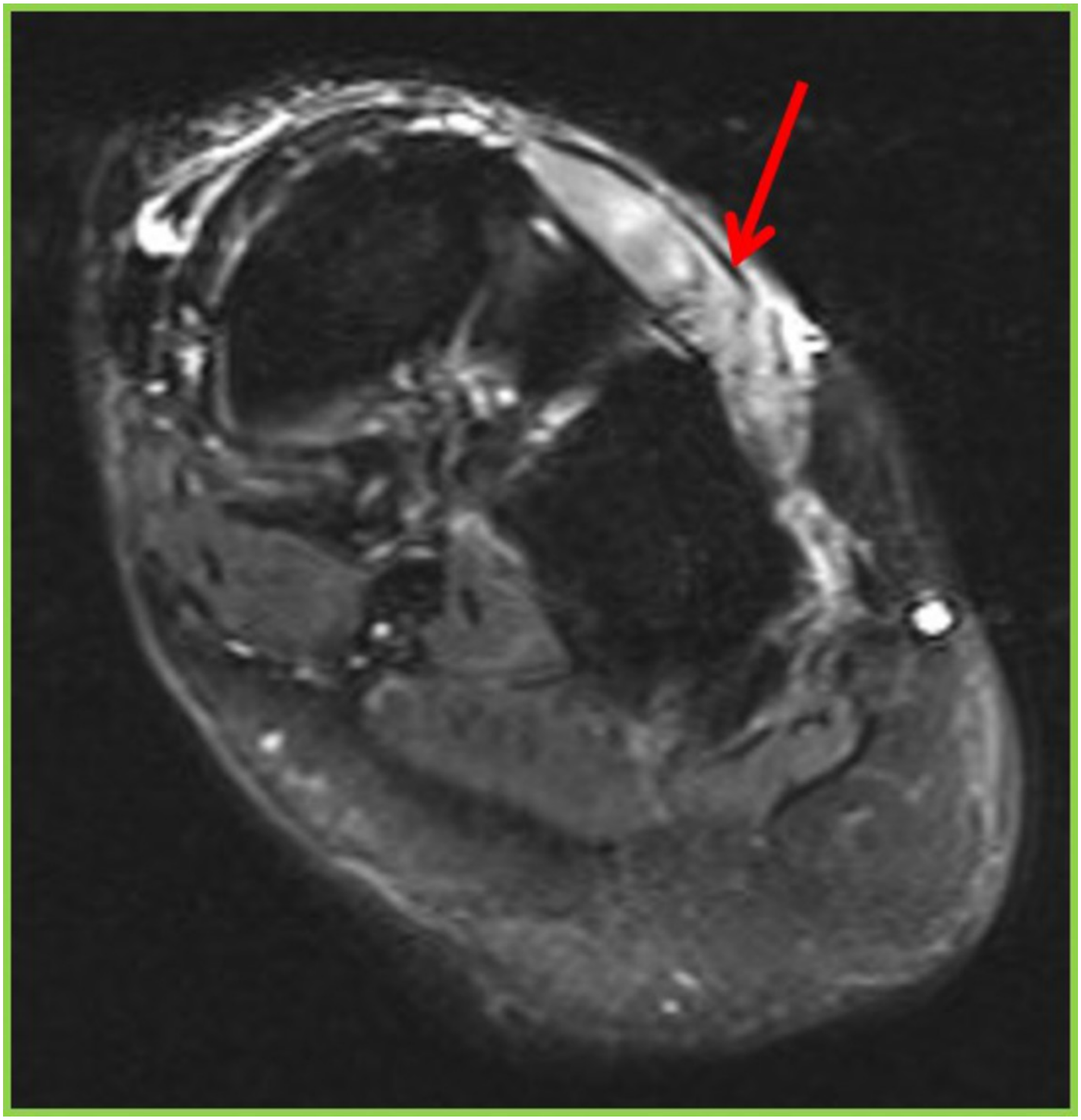

Fig. 24: Paracoronal FS T2-WI showed selective ME in the extensor digitorum brevis muscle of the left foot (arrow)


SPR

Fig. 25: Parasagittal FS T2-WI showed selective ME in the extensor digitorum brevis muscle of the left foot (arrow)

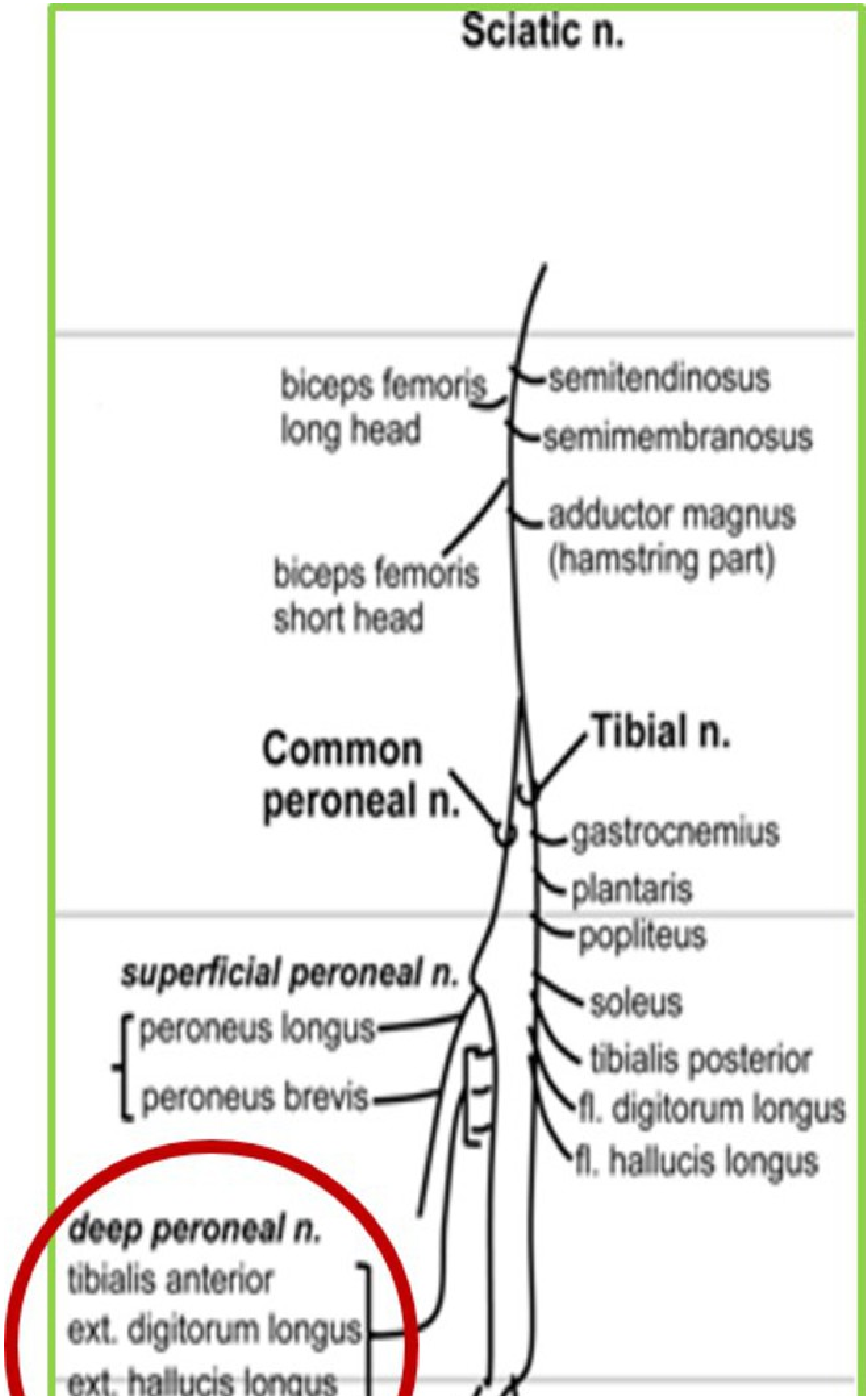
Sciatic n.
biceps femoris
long head
semitendinosus
semimembranosus
adductor magnus
(hamstring part)
biceps femoris
short head
Common
peroneal n.
Tibial n.
gastrocnemius
plantaris
popliteus
superficial peroneal n.
soleus
peroneus longus
tibialis posterior
peroneus brevis
fl. digitorum longus
fl. hallucis longus
deep peroneal n.
tibialis anterior
ext. digitorum longus
ext. hallucis longus

Fig. 26: The common peroneal nerve divides into the superficial and deep peroneal branches. The deep branch supplies the extensor muscles in the anterior compartment of the lower part of the leg, including the tibialis anterior, extensor hallucis longus, and extensor digitorum longus and (more distally) brevis muscles, whereas the superficial branch innervates the peroneus longus and peroneus brevis muscles

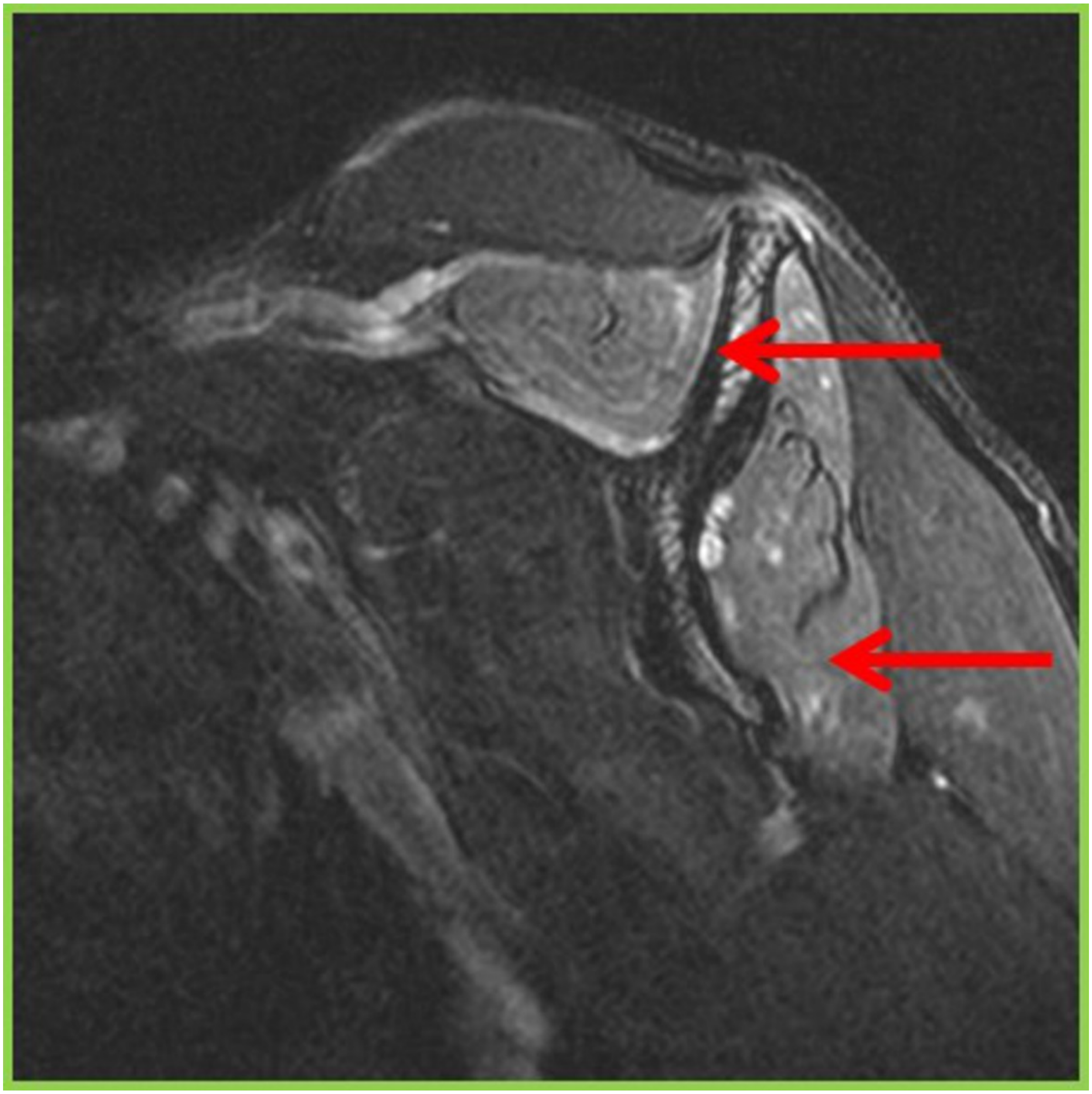

Fig. 27: Parasagittal FS T2-WI showed ME in the supra- and infraspinatus muscle (arrows)

© - Antwerp/BE

Fig. 28: Fatty atrophy (arrows) of the supra- and infraspinatus muscle is clearly depicted on parasagittal T1-WI suggestive of longer standing pathology

© - Antwerp/BE

Fig. 29: Direct MR-arthrograpy showed no evidence of a rotator cuff tear

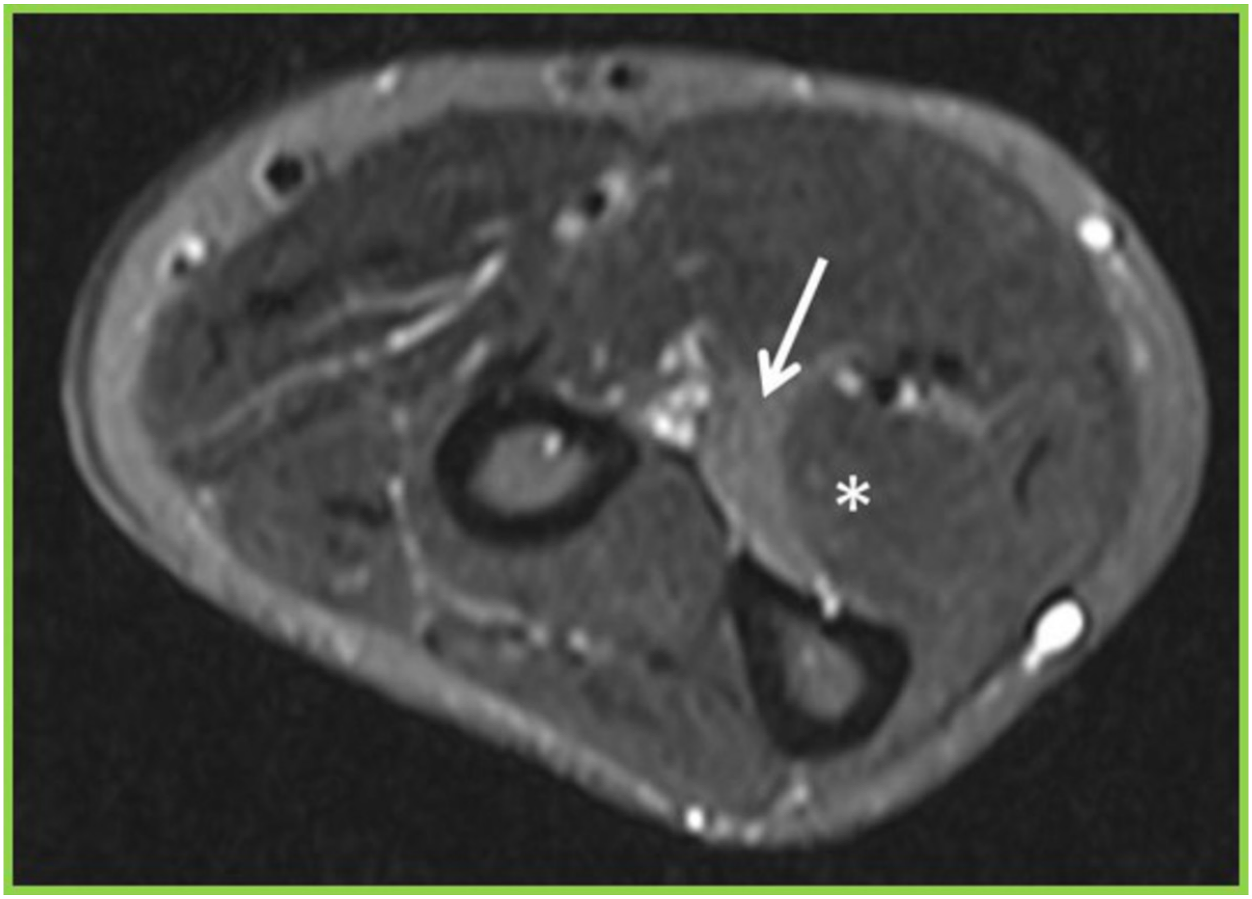

Fig. 30: Increased signal intensity is depicted on FS T2-WI in keeping with ME in the radial half of the flexor digitorum profundus (arrow), the flexor pollicis longus and the pronator quadratus muscles

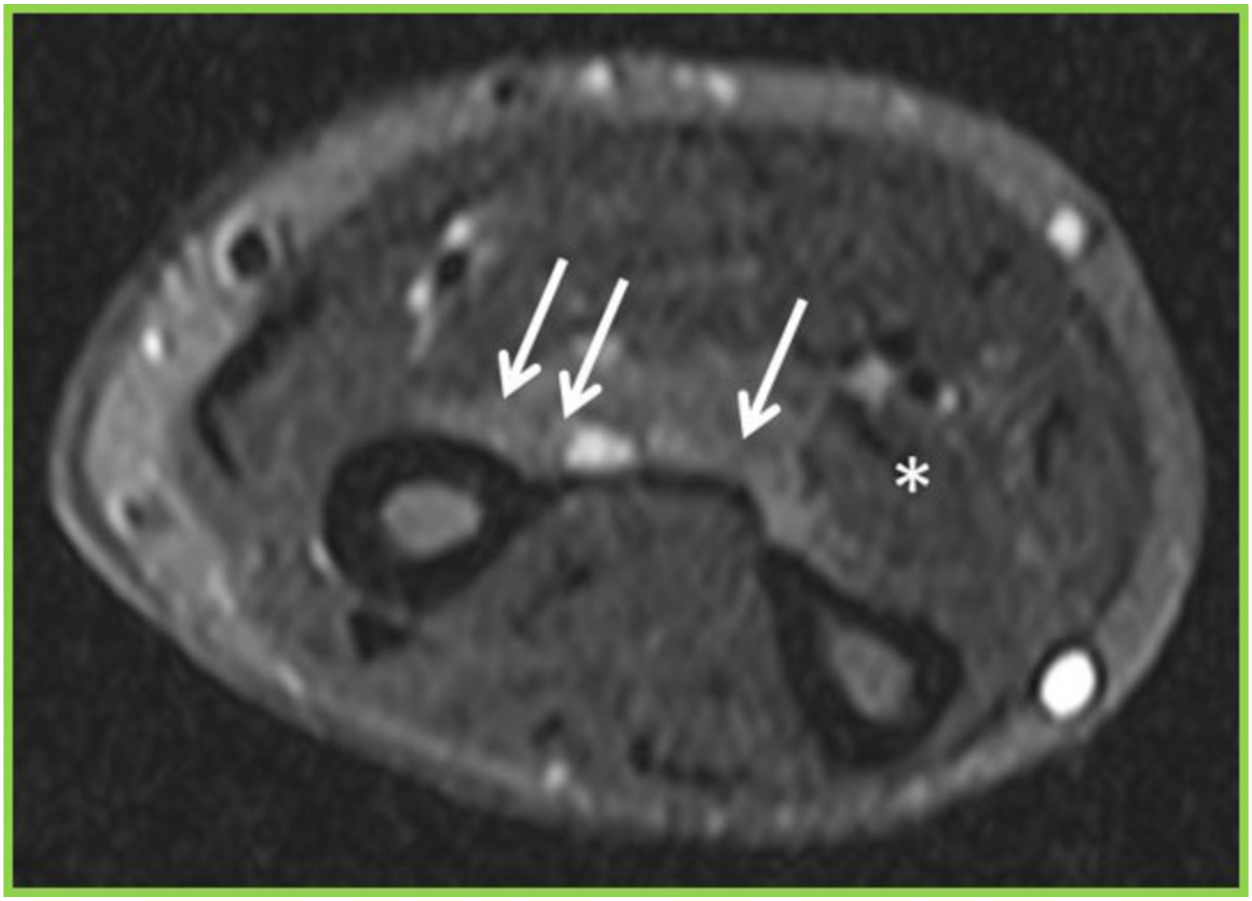

Fig. 31: Increased signal intensity is depicted on FS T2-WI in keeping with ME in the radial half of the flexor digitorum profundus (arrow), the flexor pollicis longus (double arrow) and the pronator quadratus muscles

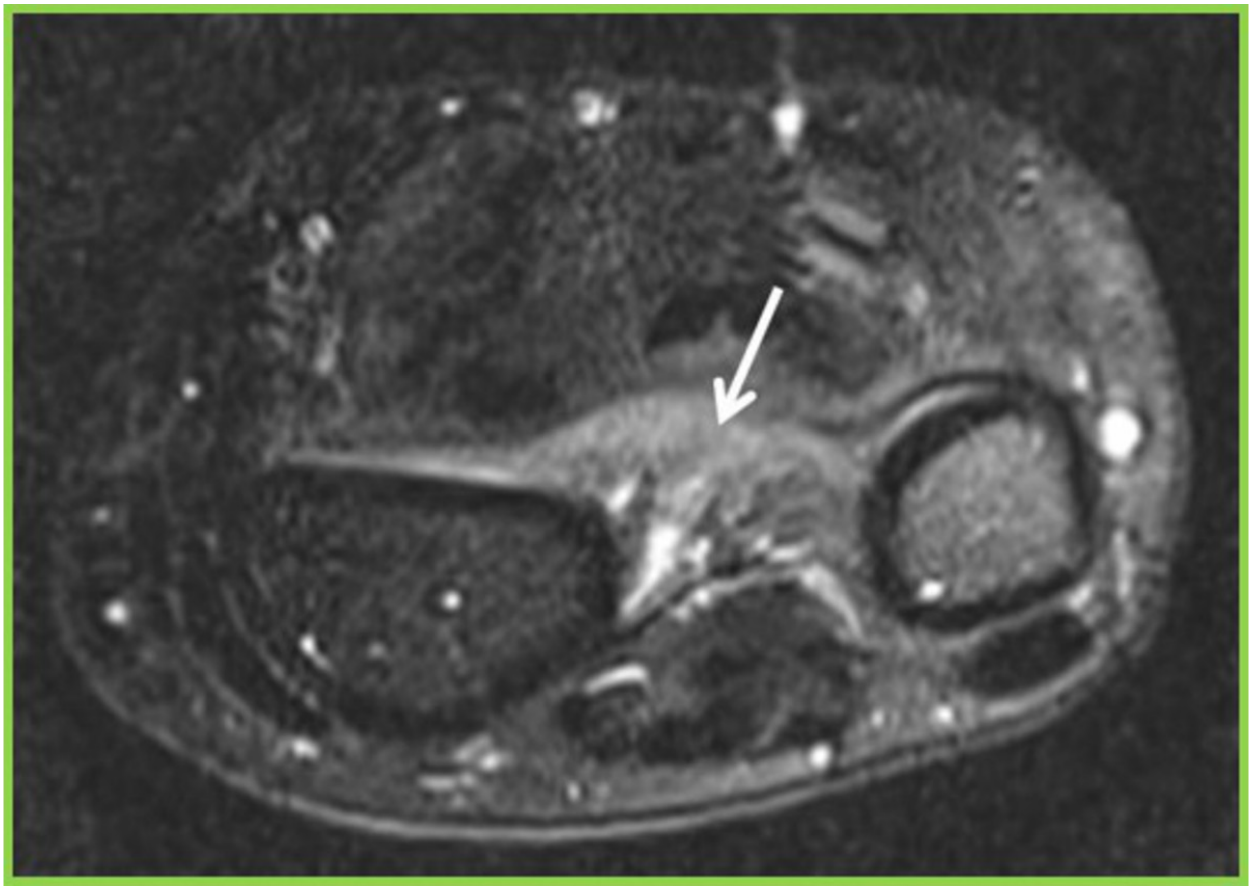

Fig. 32: Increased signal intensity is depicted on FS T2-WI in keeping with ME in the radial half of the flexor digitorum profundus, the flexor pollicis longus and the pronator quadratus muscles (arrow)

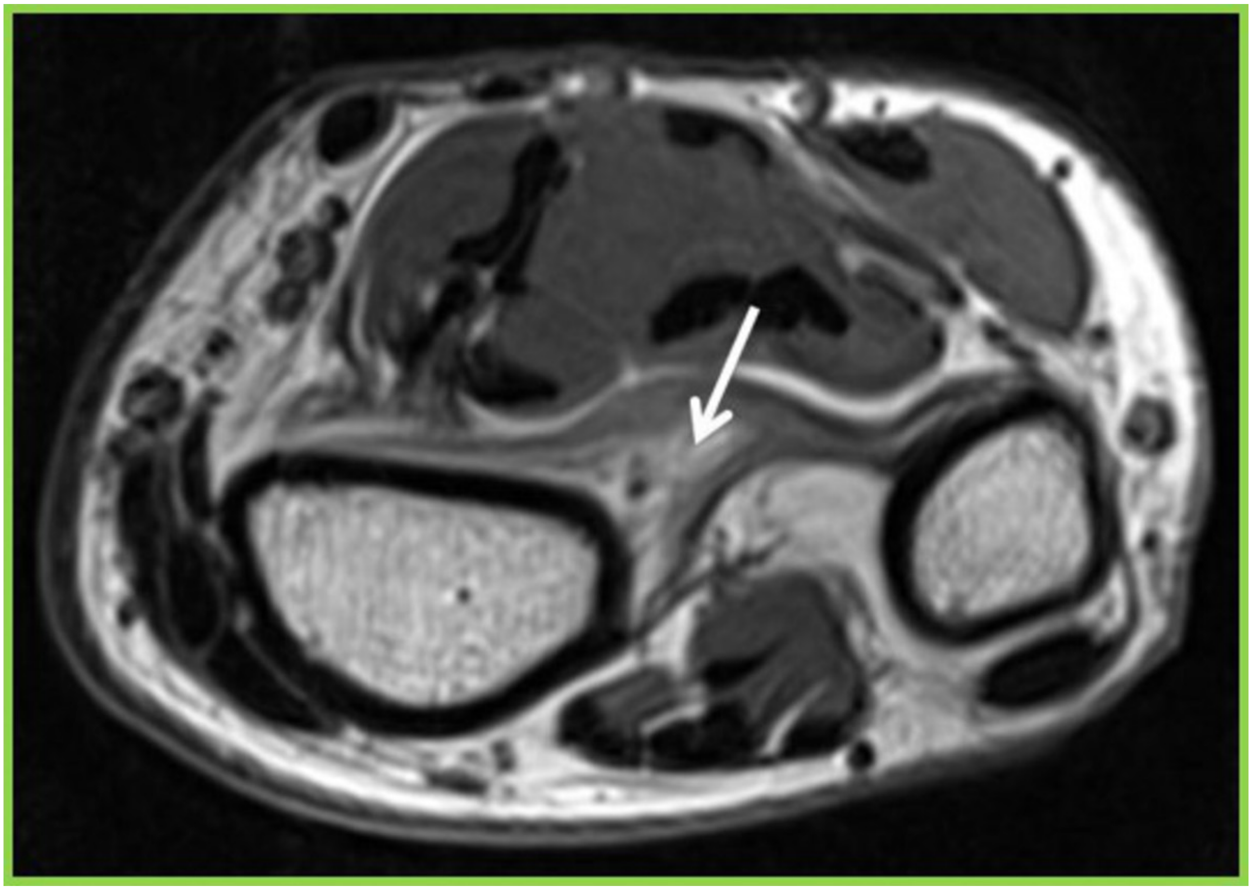

Fig. 33: Fatty infiltration and atrophy of the pronator quadratus muscle is best seen on the T1-WI (arrow)

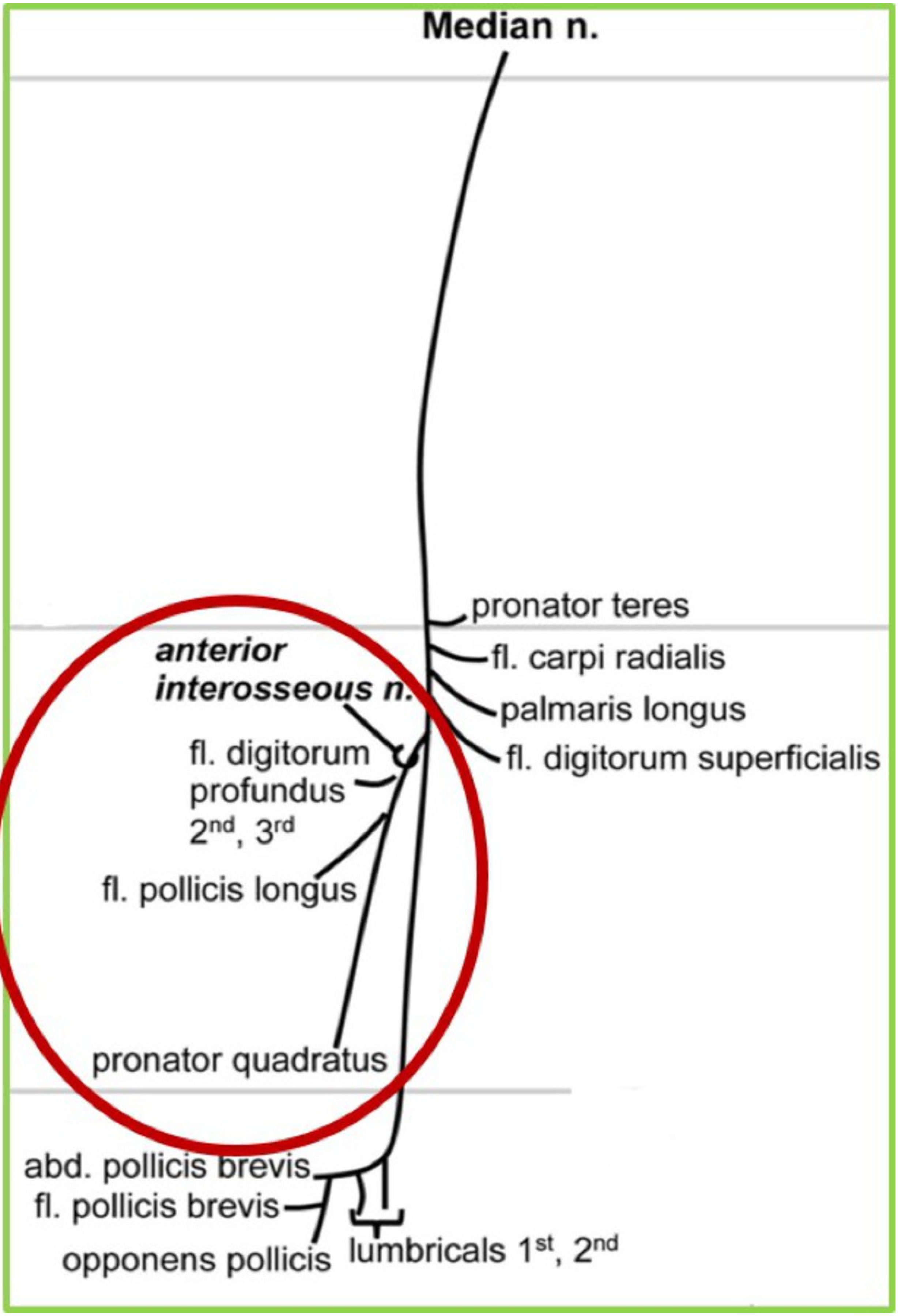
Median n.
pronator teres
fl. carpi radialis
palmaris longus
fl. digitorum superficialis
anterior interosseous n.
fl. digitorum profundus 2nd, 3rd
fl. pollicis longus
pronator quadratus
abd. pollicis brevis
fl. pollicis brevis
opponens pollicis
lumbricals 1st, 2nd

Fig. 34: The AIN is a motor branch to the deep ventral muscles of the forearm originating from the median nerve approximately 8 cm distal to the lateral epicondyle. This branch innervates the flexor pollicis longus, the radial half of the flexor digitorum profundus and the pronator quadratus muscles

© Andreisek G et al. (2006) Peripheral neuropathies of the median, radial, and ulnar nerves: MR imaging features. Radiographics 26:1267-87

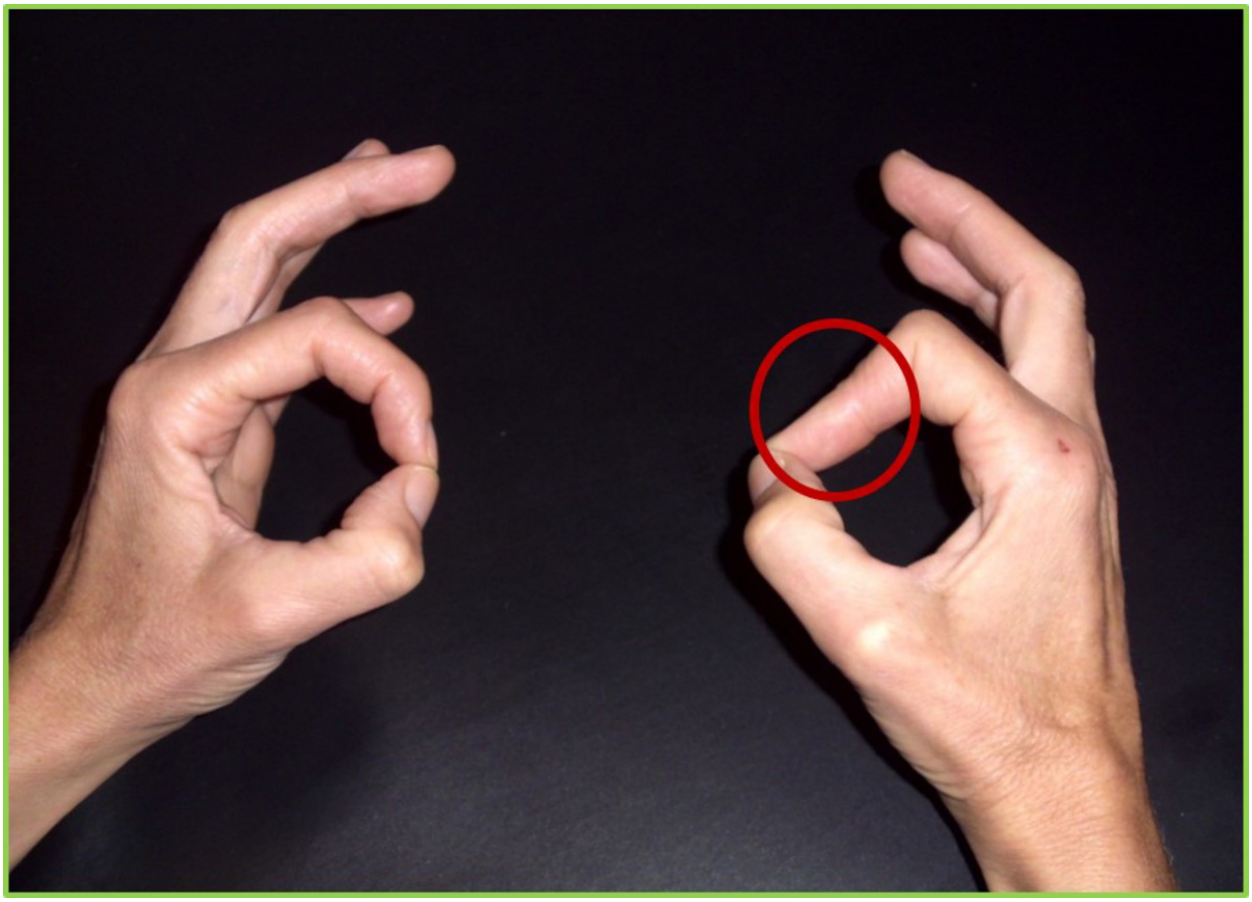

Fig. 35: Flexion at the interphalangeal joint of the thumb and the distal interphalangeal joint of the index finger is not possible due to lack of innervation of the flexor pollicis longus or flexor digitorum profundus muscles on the right side

© - Antwerp/BE

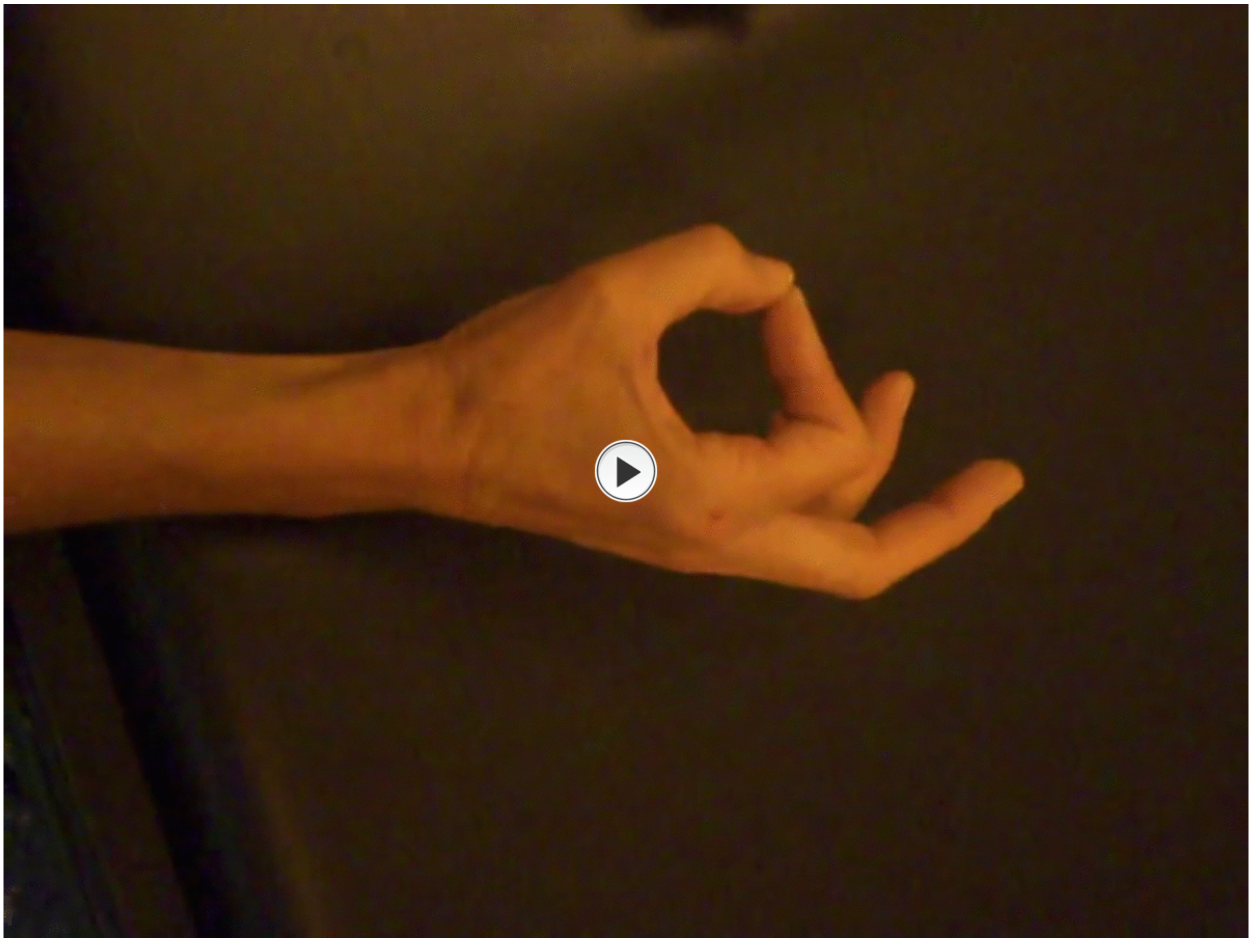

Fig. 36: Flexion at the interphalangeal joint of the thumb and the distal interphalangeal joint of the index finger is not possible due to lack of innervation of the flexor pollicis longus or flexor digitorum profundus muscles on the right side

Conclusion

The two most frequent etiologies of ME are traumatic and denervation. The focal ME pattern is mostly seen, which is in line with the preponderance of the traumatic etiology of ME in our series. FS T2-WI and T1-WI are complementary sequences in the acute and chronic stage. T1-WI are most helpful in case of denervation edema. They may add additional information regarding chronicity and reversibility.

Personal information

Michiel Eyselbergs, MD

Fellow, Department of Radiology, Antwerp University Hospital (UZA), Antwerp, Belgium, michiel.eyselbergs@telenet.be

Filip M. H. Vanhoenacker, MD, PhD

Staff radiologist musculoskeletal imaging group, Department of Radiology, Antwerp University Hospital (UZA) and Department of Radiology, AZ Sint-Maarten (Duffel-Mechelen), Antwerp, Belgium

Marguerite Faure, MD

Resident, Department of Radiology, Antwerp University Hospital (UZA), Antwerp, Belgium

Jef Huyskens, MD

Staff radiologist neuro- and musculoskeletal imaging group, Department of Radiology, Antwerp University Hospital (UZA), Antwerp, Belgium

Paul M. Parizel, MD, PhD

Professor and Chair, Department of Radiology, Antwerp University Hospital (UZA) and University of Antwerp (UA), Antwerp, Belgium

References

May DA, Disler DG, Jones Q, Balkissoon AA and Manaster BJ: Abnormal signal intensity in skeletal muscle at MR imaging: patterns, pearls, and pitfalls. *Radiographics*, 2000, 20 Spec No: S295-315.

McMahon CJ, Wu JS and Eisenberg RL: Muscle edema. *AJR*, 2010, 194: W284-92.

Andreisek G, Crook DW, Burg D, Marincek B and Weishaupt D. Peripheral neuropathies of the median, radial, and ulnar nerves: MR imaging features. *Radiographics*, 2006, 26:1267-87.

Vanhoenacker FM and Wauters T: Kiloh-Nevin syndrome. *JBR-BTR*, 2009, 92:304.

Schollen W, Degreef I and De Smet L: Kiloh-Nevin syndrome: a compression neuropathy or brachial plexus neuritis. *Acta Orthop Belg*, 2007, 73:315-8.

Eyselbergs M, De Vuyst D, Pals P and Vanhoenacker FM: Kiloh-Nevin syndrome. *Eurorad*, 2011, URL: http://www.eurorad.org/case.php?id=9784.